

Stellar Kinematic Groups II. A Re-Examination of the Membership, Activity, and Age of the Ursa Major Group

Jeremy R. King and Adam R. Villarreal¹

*Department of Physics, University of Nevada Las Vegas
4505 Maryland Parkway, Las Vegas, NV 89154-4002*

`jking@physics.unlv.edu; adamv@physics.arizona.edu`

David R. Soderblom

Space Telescope Science Institute, 3700 San Martin Drive, Baltimore, MD 21218

`drs@stsci.edu`

Austin F. Gulliver²

Department of Physics, Brandon University, Brandon, MB R7A 6A9, Canada

`gulliver@brandonu.ca`

Saul J. Adelman²

Depart of Physics, The Citadel, 171 Moultrie Street, Charleston, SC 29409-0270

`adelmans@citadel.edu`

ABSTRACT

Utilizing *Hipparcos* parallaxes, original radial velocities and recent literature values, new Ca II H&K emission measurements, literature-based abundance estimates, and updated photometry (including recent resolved measurements of close doubles), we revisit the Ursa Major moving group membership status of some

¹Present address: Department of Physics, University of Arizona, PO Box 210081, Tucson, AZ 85721

²Guest Investigator, Dominion Astrophysical Observatory, Herzberg Institute of Astrophysics, National Research Council of Canada

220 stars to produce a final clean list of nearly 60 assured members based on kinematic and photometric criteria. Scatter in the velocity dispersions and H-R diagram is correlated with trial activity-based membership assignments, indicating the usefulness of photometric- and chromospheric emission-based criteria to examine membership. Closer inspection, however, shows that activity is considerably more robust at *excluding* membership, failing to do so only for $\leq 15\%$ of objects, and perhaps considerably less. Our UMa members demonstrate non-zero vertex deviation in the Bottlinger diagram, behavior seen in older and recent studies of nearby young disk stars and perhaps related to Galactic spiral structure. Comparison of isochrones and our final UMa group members indicates an age of 500 ± 100 Myr, some 200 Myr older than the canonically-quoted UMa age. Our UMa kinematic/photometric members’ mean chromospheric emission levels, rotational velocities, and scatter therein are indistinguishable from values in the Hyades and smaller than evinced by members of the younger Pleiades and M34 clusters, suggesting these characteristics decline rapidly with age over 200-500 Myr. None of our UMa members demonstrate inordinately low absolute values of chromospheric emission, but several may show residual fluxes a factor of ≥ 2 below a Hyades-defined lower envelope. If one defines a Maunder-like Minimum in a *relative* sense, then the UMa results may suggest that solar-type stars spend 10% of their entire main-sequence lives in periods of precipitously low activity—consistent with estimates from older field stars. As related asides, we: note six evolved stars (among our UMa non-members) with distinctive kinematics and lying along a 2 Gyr isochrone that appear to be late-type counterparts to disk F-stars defining intermediate-age star streams in previous studies; identify a small number of potentially very young but isolated field stars; note that active stars (whether UMa members or not) in our sample lie very close to the solar composition zero-age main-sequence unlike Hipparcos-based positions in the H-R diagram of Pleiades dwarfs; and argue that some extant transformations of activity indices are not adequate for cool dwarfs, where Ca II infrared-triplet emission seems to be a better proxy than H α -based values for Ca II H&K indices.

Subject headings: Galaxy: kinematics and dynamics — open clusters and associations: individual (UMa group) – stars: kinematics, distances, late-type

1. Introduction

Despite a bevy of work by the late Olin Eggen arguing for the existence of stellar moving groups, the idea of kinematically-identifiable relic assemblages of otherwise unremarkable field stars sharing a common origin and earlier history remains a curiously controversial one. On the one hand, the very idea of cluster/association dissolution seems a reasonable one on its face. Open clusters confidently dated as older than the solar-age are rare, with an exhaustive list presently being Berkeley 17 (~ 12 Gyr; Phelps 1997), NGC 188 (~ 7 Gyr; Sarajedini et al. 1999), and NGC 6791 (~ 8 Gyr; Chaboyer et al. 1999). Indeed, it has been known for several decades that cluster lifetimes in the Galactic disk are typically a few hundred million years Wielen (1971). Theoretical calculations considering the disruption of star clusters due to internal relaxation, tidal effects of the stationary Galactic field, and encounters with massive objects (e.g., Giant Molecular Clouds) corroborate such empirical estimates Wielen (1991). This body of evidence seems consistent with the view of a typical Galactic disk stars forming in an associations or cluster, but eventually taking up residence in the general field (Pudritz 2002). In this picture, moving groups are viewed as a segue whose stellar denizens retain distinctive kinematic signatures expected from the slow diffusion of former clusters’ stellar orbits Wielen (1977).

On the other hand, however, much criticism has been leveled at the idea of stellar moving groups— particularly, though not exclusively, old ones; such entities have been questioned on various grounds: the true uniformity of individual stellar properties, the *a priori* nature of assumptions sometimes used to identify group members, and data/bookkeeping issues (e.g., Taylor 2000 and references therein). Recent work has placed stellar moving groups on considerably firmer footing. Several *Hipparcos*-based studies utilizing non-parametric analyses (requiring no *a priori* assumptions concerning the extent of groups’ 3-d kinematic, age, and spatial phase space) have found numerous significant phase space density enhancements above those of the general disk field population (Asiain et al. 1999; Chereul et al. 1999; Skuljan et al. 1999); many of these detected structures correspond to Eggen’s previously proposed kinematic groups, streams, and superclusters. More importantly, some of these analyses “detect” (as they should) known real structures such as the Pleiades.

Ursa Major, residing in Eggen’s proposed Sirius supercluster (Eggen 1992), has received considerable historical attention amongst putative moving groups. As noted by Soderblom & Mayor (1993; hereafter, SM93), UMa is a “best case” moving group. Its kinematics are distinctive compared to the young and intermediate age disk field. Moreover, its relatively young age (0.3 Gyr according to SM93) has likely led to the intriguing circumstance that it contains a verifiable nucleus, albeit sparse. Given the previous UMa-oriented studies of Soderblom & Clements (1987) and Soderblom & Mayor (1993), and the recent non-

parametric *Hipparcos*-bases studies noted above, we take the reality of the UMa moving group as established.

Our purpose here is to reinvestigate the membership of the UMa moving group. In doing so, we utilize new parallaxes, radial velocities, activity measures, and resolved photometry of close doubles not available to Soderblom & Mayor (1993), and consider a larger sample of candidate members than the recent study of Montes et al. (2001). We selected most candidate members from the previous UMa group studies of Soderblom & Mayor (1993) and Montes et al. (2001) (and sources therein); a few others were included based on suggested possible UMa membership mentioned in other non-UMa dedicated literature studies (e.g., Gaidos et al. 2000). The analysis was carried out with three major goals in mind. First, we wished to identify very clean samples of UMa group members and non-members that could be employed in future spectroscopic studies (or for refining extant ones) addressing the chemical homogeneity of moving groups. In doing so, 2 compromises are made: many stars are deemed to have uncertain membership status, and the necessity of adopting *a priori* kinematic definitions of the UMa group (based upon the sparse nucleus) biases the resulting kinematic statistics. Second, we wished to revisit the age determination of the UMa group using our membership list and new stellar isochrones. Third, we wished to investigate questions about chromospheric activity in UMa group stars motivated by the previous studies of Soderblom & Clements (1987) and Soderblom & Mayor (1993)—namely, is activity a robust membership indicator? How does the overall level and spread of chromospheric emission in the UMa group compare to that in older and younger clusters? An important secondary goal was to investigate the coherence of kinematic and photometric membership criteria and chromospheric activity; this has import for future use of combined criteria in investigating membership in other moving groups as well as for the reality of moving groups themselves.

2. Data

2.1. New Radial Velocity Data

Radial and rotational velocities of candidate UMa group B, A, F, and a few later spectral type stars north of $\delta = -15^\circ$ were measured from CCD spectrograms centered at 4520 Å having two-(15 μm) pixel resolution of $R \sim 60,000$. These were obtained with the long camera of the 1.22-m telescope of the Dominion Astrophysical Observatory using the 1752×532 thinned UV-coated SiTe-2 CCD, which yielded spectra of 63 Å in extent. The observations were made as either one S/N= 200 exposure or as a several observations each of lower S/N. In addition to the program stars, nightly spectra of one or more of the early radial velocity standards from Fekel (1991) were also obtained.

Each reduced (bias-subtracted, flat-fielded, dispersion-corrected, and extracted) stellar spectrum was cross-correlated with the most appropriate template spectrum using the program VCROSS (Hill & Fisher 1986). These template spectra, which covered the 4520 Å region, were calculated with the program SYNTHE (Kurucz & Avrett 1991) using Kurucz (1993) ATLAS9 solar composition models with $\log g = 4.0$ and a microturbulence of 2 km s^{-1} . For every 500 K between 14000 K and 5000 K, such spectra were calculated for rotational velocities from 10 to 40 km s^{-1} in steps of 10 km s^{-1} .

The effective temperature of each star was estimated from the mean *uvby* β photometry of Hauck & Mermilliod (1980) using the program of Napiwotzki et al. (1993) or from the spectral type if accurate photometry was not available. For each star, a template spectrum at an effective temperature given above was chosen to match the estimated temperature. In choosing an appropriate broadening for a template, two opposing requirements were considered. First, the width of the cross-correlation function should not be unnecessarily broadened and, second, the noise in the cross-correlation function generated by the stellar spectrum should be reduced by increasing the template broadening. In practice, templates were broadened by increasing amounts from a minimum of 10 km s^{-1} up to a maximum of 40 km s^{-1} for stars with the greatest $v \sin i$.

The cross-correlation functions were fitted with the appropriate Gaussian or rotational profile in a consistent manner. The centroid and width were allowed to vary but the slope of the fit was fixed at zero, an important restriction. A similar procedure was followed for the velocity standards. The standard stars used, plus their mean velocities and errors, are shown in Table 1. Two of the stars from Fekel (1991), 22 Dra and τ Her, were not used because of asymmetric cross-correlation functions.

Tab. 1

Based upon the range in corrections and the errors noted in Table 1, the decision was made not to apply any zero point shift to adjust the DAO velocity system. In part, this was also based on the suspicion that the radial velocity of o Peg may be variable. Fekel (1991) gives 7.7 and 8.5 km s^{-1} for θ Leo and o Peg, respectively, while Adelman (1988) measured 7.5 and 9.1 km s^{-1} , respectively, from DAO 2.4 Å/mm^{-1} photographic spectra. Grenier et al. (1999) find $+3.6 \text{ km s}^{-1}$ for o Peg based on seven measurements; the inferred $\sim 5 \text{ km s}^{-1}$ dispersion in their measures seems large for this relatively sharp-lined A star. With an estimated error of 0.5 to 1.0 km s^{-1} in our measures, this indicates good agreement for θ Leo; however, we suspect o Peg may be a spectroscopic binary.

The individual radial velocities are given in Table 2 along with the HJD of the midpoint of each exposure. The mean velocities given have either an internal error estimated from the fit to the cross-correlation function when only one spectrum is available or an external mean error (standard deviation of the mean) plus a mean internal error when more than

one is available. While the external mean error is to be preferred when available, for those stars with limited measures or measures confined to a single night, we adopted the generally larger internal error in order to be conservative.

Tab. 2

2.2. Kinematics

Space motions (U , V , W) and their uncertainties were derived with the version of the code used by Johnson & Soderblom (1987), but updated for J2000 coordinates and to include covariance terms in the error matrices. This was accomplished using *Hipparcos* parallaxes and uncertainties, proper motions and uncertainties from the PPM Catalogues (e.g., Bastian & Roeser 1993), and final radial velocities. These data, and relevant notes, are given for each star in Table 3. Sources of the tabulated radial velocities are (in no particular order): our new measurements, previous measures given in Soderblom & Mayor (1993), values from the more recent radial velocity catalogues of Barbier-Brossat & Figon (2000) and Duflot, Figon & Meyssonnier (1995), and precision values from the literature. In most cases, catalogue values replaced the SM93 values unless the latter were their precision CORAVEL results.

Tab. 3

Uncertainties in the catalogue velocity values are frequently qualitative. Reasonable adopted numerical values were arrived at by comparison of quality flags and numerical uncertainties for those stars having both, taking into account the number of observations. Comparison of different measurements for stars not identified as a binaries indicate pleasing agreement— typically within 1.5 km s^{-1} or better. A few discrepant values (e.g., those for HD 27861, 111456, 148112AB, 205765AB, 206538A, 209515AB, and GJ625) suggest continued benefit from additional measurements and/or monitoring. Variance weighted mean radial velocities from the differing sources were determined for each star; these were utilized to determine final UVW kinematics and their formally propagated uncertainties, which are listed in Table 4.

Tab. 4

2.3. Photometry

Precision photometry (V magnitudes, and $B - V$ and $V - I$ colors) and uncertainties were extracted from the *Hipparcos* and *Tycho* catalogues, and are listed in Table 5 along with the absolute magnitudes derived from the *Hipparcos* parallaxes. In cases where these data were absent or unusually uncertain or possibly contaminated by close components, literature photometry was drawn upon. Of particular note is the new Tycho-based photometry of close doubles provided by Fabricius & Makarov (2000). Their V_T magnitudes and $B_T - V_T$

colors were transformed to Johnson V and $B - V$ using the relations from Bessell (2000). Reliable photometry for close components can provide additional photometric constraints on evolutionary status, and represents a significant improvement over previous membership studies.

2.4. Metallicities

Fe abundances were taken from the catalogues of Cayrel de Strobel (1997, 2001), and are provided in Table 5 along with the formal dispersion (standard deviation) of multiple measurements. In cases of two measurements, the range is indicated; no uncertainty estimate is given for single measurements. Older measurements with (rightly or wrongly) perceived lesser reliability are flagged with a ‘?’ . We acknowledge that the tabulated values are probably inhomogeneous, and no attempt has been made to rectify this. Such an attempt is not practically accomplished either empirically (due to lack of overlap between different studies) or fundamentally (due to implicit differing assumptions in the analyses such as choice of model atmospheres, temperature scales, atomic data, solar normalization, etc. which are impossible to calibrate).

2.5. Activity Indicators

Residual chromospheric flux ratios of Ca II H&K are also provided in Table 5. These are predominantly new Kitt Peak National Observatory coude feed-based values from DRS and JRK’s ongoing study of chromospheric activity in nearby stars, though a few measures have been taken from the literature. The ‘*additional candidates*’ lack Ca II-based measures. For all other objects, the lack of an entry signals that the activity measures from SM93 were utilized.

Tab. 5

3. Results

3.1. Activity-Based Classifications

For consistency with SM93’s activity divisions, we divided the sample into different categories (Probable Spectroscopic Members, Possible Spectroscopic Members, Probable Spectroscopic Non-members, and Additional Candidates)) using chromospheric activity measures. This was done to investigate the relationship between other membership criteria and

activity measures, rather than using the activity as a criterion proper. Thus, we can later use our final memberships to investigate chromospheric activity scatter in the UMa group without recourse to circular argumentation. Below, we infer an UMa cluster/group age of $\sim 500 \pm 100$ Myr, intermediate to the well-studied Hyades and M34 open clusters having canonical ages of 800 and 200 Myr. As we later show, comparison of UMa group candidate stars' with these clusters' activity distributions can efficiently exclude UMa group non-members, and provide confirmation of apparent members. Given our ongoing Ca II H&K study of several thousand nearby stars noted above, we have chosen Ca II H&K as our activity indicator.

Soderblom, Jones & Fischer (2001) present $H\alpha$ and $\lambda 8498$ Ca II infrared triplet (IRT)-based activity measures for a large selection of M34 dwarfs in their Table 1. These have been transformed to $\log R'_{HK}$ values using the regressions deduced from Figures 3 and 4 of Herbig (1985):

$$R_{HK} = 2.725 \times R_{H\alpha} + 1.35 \times 10^{-6} \quad (3-1)$$

and

$$R_{HK} = 5.102 \times R_{8498} - 5.00 \times 10^{-6} \quad (3-2)$$

The transformed $H\alpha$ -based $\log R'_{HK}$ values are plotted versus the transformed Ca II IRT-based values in Figure 1a. The correlation coefficient is significant at the $> 99.9\%$ confidence level, and ~ 0.2 dex mean offset noted for UMa candidates by SM93 is apparently present, as is considerable scatter of ~ 0.25 dex about a mean relation. While SM93 simply made a 0.2 dex adjustment to the IRT-based values, this is not the optimum procedure for M34. Figure 1b shows the difference between the transformed IRT- and $H\alpha$ -based M34 measures versus dereddened color, and indicates a significant portion of the scatter in Figure 1a is correlated with color.

Fig. 1

The trend in Figure 1b was fit with a third order Legendre polynomial using 2.0σ -clipping. The power series expansion of the fit (shown as the dotted line in Figure 1b) is given by

$$\Delta \log R'_{HK} = -5.0506 \times 10^{-1} + (1.7352 \times (B - V)) - (1.5453 \times (B - V)^2) \quad (3-3)$$

Curiously, the same color-dependent difference is not seen for the UMa data from SM93. The difference between these transformed $H\alpha$ - and IRT-based activity measures is plotted versus color in Figure 1c. The correlation coefficient suggests the positive slope is marginally significant (92.5% confidence level); if real, it is opposite in sign to that for the M34 data in Figure 1b. These differences must be intrinsic ones or due to measurement since the transformations are the same. Figure 1d shows transformed $H\alpha$ -based $\log R'_{HK}$ values that have been corrected using equation 3-3 from the fit in Figure 1b versus the Ca II IRT-based

values; reduced scatter about the one-to-one relation is readily evident. We explicitly note here that our choice has been to correct the $H\alpha$ -based activity measures onto the Ca II IRT-based scale; this is different than SM93’s procedure, and is not an arbitrary decision (see the appendix).

Figure 2 displays the situation for ~ 100 Myr-old Pleiades dwarfs whose $H\alpha$ - and $\lambda 8542$ Ca II IRT-based data come from Soderblom et al. (1993); these measures were transformed as before, except using the relation for the $\lambda 8542$ feature deduced from Herbig’s (1985) Figure 4:

$$R_{\text{HK}} = 2.939 \times R_{8542} - 5.00 \times 10^{-6} \quad (3-4)$$

The deviation from a one-to-one relation between the transformed activity indicators (Figure 2a) is similar to that demonstrated by the M34 data. The Pleiades differences are also a function of color as shown in Figure 2b, where the solid line indicates the fitted quadratic relation:

$$\Delta \log R'_{\text{HK}} = -4.2440 \times 10^{-1} + (1.4977 \times (B - V)) - (1.2465 \times (B - V)^2) \quad (3-5)$$

that is similar to equation 3-3 for M34 (dotted line) in Figure 1b. The more satisfactory state of affairs upon correcting the $H\alpha$ -based values to the Ca II IRT scale can be seen in Figure 2c.

Fig. 2

Figure 3 shows the mean of the transformed IRT- and *corrected* $H\alpha$ -based values versus dereddened $(B - V)$ color for M34 (crosses) and Pleiades (open circles) dwarfs. Here, the $H\alpha$ values have been corrected onto the IRT scale using the fitted relation for the Pleiades dwarfs (Figure 2b) for both the Pleiades and M34 stars– with the reasoning that the more numerous Pleiades data result in a better determined mean relation given the significant star-to-star scatter (Figure 1b). The filled circles are the *directly measured* Pleiades H&K indices from Soderblom et al. (1993); these are connected to the transformed values for six stars in common. The solid line and dotted lines depict the mean Hyades relation and the full extent of its scatter from direct H&K measurements in Soderblom (1985); the flatness of the relation for $(B - V) \geq 0.85$ was not derived from Hyades data, but simply argued for by Soderblom (1985); however, the flatness in the *directly measured* $\log R'_{\text{HK}}$ values for similarly cool Pleiades stars seems consistent with this.

Fig. 3

The lower envelope to the M34 data may show an unexpected decline with increasing color; utilizing the specific M34-based corrections from Figure 1b actually exacerbates (slightly) this trend. Such a trend could suggest the IRT- $H\alpha$ corrections are not as steep a function of color as for the Pleiades. Thus, the color dependence of the relative robustness of the transformed IRT and $H\alpha$ indices as proxies for the Ca II H&K index may be activity or age-dependent. While a seemingly elaborate explanation, this is consistent with the near

lack of a color-dependent difference for the older UMa objects in Figure 2b, and the consistency (essentially forced in order to yield our transformations) of the less active field stars from Herbig (1985).

For our purposes, there are several notable features about Figure 3. First, the vast majority of the younger M34 and Pleiades stars lie above the mean Hyades relation; essentially all of the Pleiads do for $(B - V) \geq 0.8$. Second, the spread in activity for the younger M34 and Pleiades stars is significantly larger than for the older Hyades dwarfs. We have thus followed SM93’s approach in assigning a provisional activity-based membership classification to our objects where possible. Those apparently single objects which lie within a few hundredths of a dex or above the Hyades relation are classed as ‘*probable spectroscopic members*’. Close binaries which meet the same criterion are deemed ‘*possible spectroscopic members*’ (since large levels of activity may be related to binarity), as are apparently single objects lying significantly beneath the mean Hyades relation but within the Hyades scatter. Other objects are considered ‘*probable spectroscopic non-members*’. Objects not having chromospheric emission measurements are referred to as ‘*additional candidate members*’. The scatter in Figure 3 should also prepare one for occasionally encountering objects with sub-Hyades activity that might be younger *bona fide* UMa members.

3.2. UMa Nucleus Stars

Our new $\log R'_{\text{HK}}$ values for four canonical UMa nucleus stars (listed in Table 5) are in good accord with the average SM93 values; the deviations (in the sense new–SM93) are -0.08 , -0.19 , -0.10 , and -0.08 dex. While a slight ~ 0.1 dex offset may be present, the new activity indicators still indicate probable spectroscopic membership; even though the indices for HD 109011, 109647, and 110463 lie a couple hundredths of a dex below the red end of the Hyades relation, they are well within the small Hyades scatter. Moreover, the preponderance of other activity measurements (SM93) suggests probable spectroscopic membership using the mean Hyades relation criterion.

Canonical UMa Nucleus stars are shown in the V - U and V - W kinematic planes in Figures 4a,b. The ellipse is centered on the (inverse variance-) weighted mean velocities and has semi-major and -minor axes equal to three times the respective formal rms velocity dispersions. The vital kinematic statistics for all activity-based subgroups are reported in Table 6. The weighted rms dispersions are reduced slightly (by 0.1, 0.0, 0.3 km s $^{-1}$ in UVW) compared to SM93’s results; the unweighted dispersions (a fairer comparison to SM93) are somewhat larger, however (by 0.0, 0.4, and 0.2 km s $^{-1}$ in UVW). This increase can be traced to the marginal outlier HD 111456, whose kinematic differences from SM93

values can be traced to the adopted radial velocities (adopting the *Hipparcos* proper motions, e.g., only increases differences in U and V); this illustrates the continued importance of additional radial velocity measures. Indeed, HD 111456 and the marginally outlying HD 106591 are among the few objects whose new radial velocities and previous measures disagree by considerably more than the respective errors. Excluding HD 111456, the unweighted dispersions are equivalent or slightly lower than the SM93 values.

Fig. 4

On an absolute basis, comparison of the mean UVW with the SM93 values is at the level of “fine tuning”. The mean W velocities are essentially identical, while the V velocities differ at only the $\sim 1\sigma$ level. The most significant, though small, difference is in the mean U velocity. Our $1.3\text{--}1.4\text{ km s}^{-1}$ larger value represents a $4\text{--}5\sigma$ level difference given the respective inferred mean uncertainties.

Tab. 6

Figures 4c,d contain the *Hipparcos*-based $M_V\text{--}(B - V)$ and $-(V - I)$ color magnitude diagrams of the UMa nucleus stars. Shown for comparison are the latest generation Yale isochrones (Yi et al. 2001) for 600 Myr ($B - V$) and 400 Myr ($V - I$) for both scaled solar $Z = 0.01$ and 0.02 mixtures and for both the color-temperature conversions of Lejeune et al. (1998) and Green et al. (1987). The metallicity study of Boesgaard & Friel (1990) suggests $[\text{Fe}/\text{H}] = -0.09$ for UMa, which corresponds to an intermediate $Z = 0.016$ for $Z_\odot = 0.02$. The data points form a very tight main-sequence and turn-off (reflecting the quality of the parallaxes now available), and lie close to the assumed isochrones. The $M_V\text{--}(B - V)$ data are best fit by the 600 Myr isochrones, whereas the $(V\text{--}I)$ -based data are best fit by the 400 Myr isochrones. Statistical uncertainties in these values pale in comparison to the color-based differences, which may be due to systematic errors in the photometry or the isochrones’ assumed color- T_{eff} conversions. We thus infer an UMa age of 500 ± 100 Myr, and we use the 600 Myr and 400 Myr isochrones as fiducials to evaluate photometric membership.

3.3. Membership Assignments

Kinematic, photometric, and final membership assignments are listed for all objects in Table 5. The meanings of these qualitative assessments are ‘Y’=certain membership, ‘Y?’=probable membership, ‘N?’=probable non-membership, and ‘?’=uncertain membership. The final membership assessments are conservative in the sense that the possibility of contaminating the non-members category with true members, or contaminating the member categories with true non-members was avoided at the cost of relegating objects with conflicting or questionable criteria to the uncertain category for future study. In this sense, an uncertain designation is not to be necessarily equated with a lower true membership and/or higher non-membership probability on a star-by-star basis; rather, we simply required more

consistent evidence for a definitive classification.

The V - U and V - W kinematic planes are shown in the top panels of Figures 5-8 for the *probable spectroscopic* (i.e., activity-based) *member*, *possible spectroscopic member*, *probable spectroscopic non-member*, and the *additional candidate member* (which lack activity measures) subgroups. The velocity ellipses are those of the canonical UMa nucleus stars from Figures 4a,b. A ‘Y’ kinematic membership is given those stars that fall within both planes’ ellipses. A ‘Y?’ kinematic membership is given those stars that fall within both ellipses only within the stellar kinematic uncertainties. A ‘N?’ kinematic designation is assigned those stars which lie outside both kinematic planes’ ellipses even within the stellar kinematic uncertainties; generally, this signals a significant departure from all three of canonical UMa nucleus stars’ mean UVW values. Other objects are assigned a ‘?’ designation— usually indicating contradictory findings; generally, this signals a significant departure from one or two (but not all three) of the canonical UMa nucleus stars’ mean UVW values. Photometric memberships are assigned in a similar fashion, replacing the nucleus stars’ velocity ellipses with a band of occupation through the H-R diagram outlined by the nucleus stars. For candidate objects lying outside these regions (cool dwarfs or evolved subgiants), we rely on the placement relative to the selected isochrones for guidance. The *Hipparcos*-based H-R diagrams for the different activity-based subgroups are shown in the bottom panels of Figures 5-8. The kinematic and photometric based assignments are listed in Table 5 for all objects.

Final membership assignments, also listed in Table 5, combine the kinematic and photometric results and any spectroscopic $[\text{Fe}/\text{H}]$ determinations available. Care was taken in the relative consideration of these criteria. In particular, the main use of photometric and metallicity criteria is to veto positive membership and not grant it since a warm or cool UMa non-member dwarf lying on the lower UMa main-sequence or having a near-UMa metallicity ($[\text{Fe}/\text{H}] \sim -0.09$) is hardly remarkable. In other words, photometric and abundance-based membership are necessary but far from sufficient conditions to guarantee UMa membership. Their most powerful use is in identifying non-members— particularly older disk stars that lie in the Hertzsprung gap far below the UMa subgiant branch. The H-R diagrams in Figures 6 and 7 provide illustrative examples of this.

Exceptions to this use do exist. Photometric membership near and above the UMa main-sequence turnoff is a more stringent affirmative indicator of membership since it implies, at the very least, a conspiracy of age and opacity identical to the UMa nucleus stars’. Abundance information for the A stars in our sample is, in most cases, best considered neither inclusive nor exclusive given the variety of abundance anomaly phenomena (Am, λ Boo, etc) which occur in this region of the H-R diagram. Additional leeway is given for a few stars after a careful star-by-star consideration— in particular, for those stars with

known or suspected companions that lack individual photometry or systemic radial velocity determinations. These additional considerations are conservative in the sense described above. For example, a kinematic non-member (N?) that was classified as a photometric member (Y) generally is assigned an uncertain (?) final membership, despite the fact that its kinematic non-membership designation is likely secure. In this way, possible ‘contaminants’ are relegated to the uncertain category.

Fig. 5
Fig. 6
Fig. 7
Fig. 8

4. Discussion and Comparison to Previous Results

4.1. Final Membership

The kinematic planes and H-R diagrams of the nucleus stars and those objects having final membership designations of Y and Y? are shown in Figure 9. The final mean UVW velocities are given in Table 6; the values (+14.5, +2.9, and -8.6 km s^{-1}) are within a few tenths of a km s^{-1} of the UMa Nucleus values discussed above. Our values are also in excellent agreement—typically within a couple km s^{-1} that is within the mean uncertainties deduced from the formal dispersions—with the mean kinematics deduced from the studies of Asiain et al. (1999), Chereul et al. (1999), and Orlov et al. (1995), which utilize statistically sophisticated membership identification algorithms lacking *a priori* assumptions implicitly incorporated here, and the recent study of Montes et al. (2001) employing Olin Eggen’s proper motion-based peculiar velocity and moving cluster predicted radial velocity criteria. These determinations are listed at the bottom of Table 6. The agreement given the different samples and membership criteria employed is pleasing, and perhaps lends some confidence to the reality of the UMa moving group.

Fig. 9

Inspection of the Bottlinger diagrams in Figure 9 reveals asymmetries in the U and W distributions indicative of a non-zero vertex deviation. This particular deviation and others are also seen in the recent studies of Asiain et al. (1999; their Figure 6), Chereul et al. (1999; their Figures 15 and 17), Skuljan et al. (1999; their Figures 5, 8, and 10), and Montes et al. (2001; their Figure 2); these studies cover a much larger range in the Bottlinger diagram, revealing significant structures on larger kinematic scales shown here. That nearby young disk stars exhibit non-zero vertex deviations has been known for some time (e.g., Mihalas and Binney 1981; Chapter 7), though Mihalas and Binney (1981) also note that this behavior may not be a general property of the global Galactic young disk field, but attributable to the nearby young disk field being dominated by kinematic moving groups which demonstrate significant vertex deviation. Nevertheless, an interesting question is how these “branch”-like (as opposed to elliptical) structures in the Bottlinger diagram arise for moving group stars. As suggested by Mihalas & Binney (1981), perhaps the most plausible

explanation is that they are due to a peculiar spatially- and temporally-localized convolution of the Galactic potential and velocity field at the time of these stars’ *en masse* formation—in particular, the influence of density waves related to Galactic spiral structure; Skuljan et al. (1999) suggest that their “branch-like” kinematic structures (even if of different age) in the Bottlinger diagram are related to spiral structure. Alternatively, inspection of Figures 15 and 17 of Chereul et al. (1999) might suggest that these structures may arise from the close proximity (in the Bottlinger diagram) of distinct moving groups with near-zero vertex deviation which, when merged together under coarse resolution, then take on a “branch”-like non-zero vertex deviation appearance. However, one must still ask why such distinct groups are in such proximity and in a “branch”-like configuration to begin with. Thus, this alternative explanation may, itself, simply reduce to a relation with spiral structure.

The final H-R diagrams in Figure 9 confirm our earlier Nucleus-based age estimate of 500 ± 100 Myr for the UMa group. This is in outstanding agreement with the Stromgren-photometry based estimate of 520 ± 160 Myr of early-type Sirius supercluster members identified by Asiain et al. (1999), and the 600 Myr age of the dominant Sirius supercluster component found by Chereul et al. (1999). Our age estimate is larger than the usually quoted value of 300 Myr previously assigned to the UMa cluster (e.g., SM93 and references therein) on the basis of disparate methods. Our upward revision is important inasmuch as it provides a rare age-based data point between the well-studied younger Pleiades (100 Myr; Meynet et al. 1993, Yi et al. 2001) and M34 (200 Myr; Meynet et al. 1993, Jones et al. 1997) open clusters and the slightly older (650 ± 150 Myr; Castellani et al. 2001, Perryman et al. 1998) Hyades and Praesepe (itself apparently of Hyades age; Mermilliod 1981) open clusters for age-sensitive abundance or stellar evolution studies. We acknowledge, however, that it remains to be rigorously demonstrated that these disk clusters (and others) are truly on a homogeneous age-scale.

An intriguing result of the *Hipparcos* mission was a suggested Pleiades distance modulus some 0.3 magnitudes fainter than that inferred from main-sequence fitting; controversy has erupted over whether the parallaxes or assumptions and/or details of the modeling are at fault (see, e.g., Pinsonneault et al. 1998). Soderblom et al. (1998) suggested that other such subluminous stars seemed to be absent amongst nearby young field stars identified via chromospheric emission. We find the same to be true in this work. The final UMa member H-R diagram in Figure 9 shows that the *Hipparcos*-based observed dwarf locus lies close to, but slightly beneath, the new Yale $Z=0.02$ isochrones (short and long-dashed lines); this is as expected given previous limited UMa abundance studies. A 0.3 magnitude subluminosity would place the observed locus essentially on the Yale $Z=0.01$ isochrones (solid and dotted lines), which is not the case. The same appears to be true of the probable and possible activity-based stars (whether final UMa members or not) in Figures 5 and 6. Since it seems

likely that these objects are young disk members, comparison to the Pleiades is highly relevant. In sum, our results too suggest that the Hipparcos distance problem, whatever its cause, seems to be limited to the Pleiades (and perhaps a couple other less well-studied open clusters).

The coherence between the scatter in the kinematic and H-R diagrams can be seen by comparing Figures 4-8. The photometric and kinematic discriminants seem to work together in large measure. The velocity dispersions of our nucleus stars plus stars with final Y and $Y?$ assessments are smaller than for any activity-alone based group, demonstrating that the kinematic and photometric criteria have added great value to SM93’s employment of an activity criterion. Comparison with other results (next subsection) also indicates the reliability of our results. We strongly caution readers first, though, that our velocity dispersions of the nucleus plus final member stars should *not* be taken as robust estimates of the true UMa group values—the former are certainly biased by using the UVW plane as a membership discriminant. Even with the lack of kinematic membership criteria, other subtle and insidious biases induced by measurement availability and/or initial sample selection may also be present (e.g., see the discussion Skuljan et al. 1999).

4.2. Alternative Kinematic Criteria

That the true velocity UMa group dispersions are expected to be larger than our estimates is not surprising since appreciable dispersion must exist for the group to be unbound and spatially extended in the Galactic disk. Some investigators have focussed on or heavily-weighted V motions in considering kinematic membership given dynamical calculations indicating diffusion in the UW directions leads to epicyclic oscillations of a star about these mean motions, which is not true in V (Wielen 1977; Binney & Tremaine 1987). The usefulness in using V motion as a sole or heavily-weighted kinematic criterion receives some observational support. SM93 noted that if one allowed for plausible parallax uncertainties, all their probable spectroscopic members could have V motions in agreement with the UMa nucleus mean without creating any additional spread in U and W . Moreover, examination of our final members and our activity-based spectroscopic groups in Table 6 indicates that the V velocity dispersion is significantly less than the U and W dispersions.

Despite the theoretical expectations and these observational findings, we have made no attempt at using a more restrictive V -based criterion here. This is due to three reasons. First, the dispersions of our final members are biased estimates. Second, the estimates of Asiain et al. (1999) and Chereul et al. (1999)—who use non-parametric methods which make no *a priori* assumptions regarding the mean group kinematics—listed in Table 6 do not

seem to indicate that the velocity dispersion in V is significantly smaller than that in U and W . Third, and perhaps relatedly, Chereul et al. (1999) find evidence that Eggen’s Sirius supercluster (which harbors the UMa group) can be broken down into two superclusters mostly distinguished by differing V velocity³ ($+0.7 \text{ km s}^{-1}$ versus $+4.2 \text{ km s}^{-1}$).

At the same time, it is likely that the results of these non-parametric statistical studies would refine our results in the sense that some stars classified with uncertain (?) membership due to their mildly deviant kinematics would be true *bona fide* UMa group members. This is simply because these presumably unbiased (or less biased) velocity dispersions are $5\text{--}7 \text{ km s}^{-1}$ as opposed to our 3σ dispersions of $2\text{--}3 \text{ km s}^{-1}$ from UMa nucleus stars. Montes et al. (2001) suggest even larger values from the *Hipparcos*-based wavelet analysis of stellar velocities in the solar neighborhood by Skuljan et al. (1999), whose kinematic “branches” of late-type stars in the UV plane can be measured in tens of km s^{-1} . Inasmuch as we focus on producing a list of clean assigned UMa members and have taken care to avoid wrongly classifying possible *bona fide* members as non-members, we deem the bias in our results acceptable. Interesting subgroups of stars, including possible *bona fide* members not classified as such here, are considered later.

While the recent UMa group membership study of Montes et al. (2001) uses different criteria than us to establish membership, and takes advantage of convergent points and total space velocities, their approach is not wholly independent from ours since they also employ three-dimensional velocities—proper motions and radial velocities as opposed to our transformed UVW values. Their approach may appear more quantitative, but their use of Eggen’s criteria is arbitrary to some degree since any kinematic membership cutoffs depend on a convolution of *a priori* knowledge or assumptions about intrinsic dispersion and measurement uncertainties. Given these subtle intrinsic similarities, comparison of our results is of interest; in doing so, we have included the binary stars available in the web-database of Montes et al. (2001).

The comparison of our final memberships with the kinematic results of Montes et al. (2001) is shown in the form of a contingency table in Table 7 where memberships for discrete components of the same system have been counted separately. We note that the kinematic values themselves are in outstanding agreement, and differences in our final classifications are due to those in methodology. In the case of exact agreement, the 3×3 contingency table formed by the top 3 rows and final 3 columns would be dominated by the diagonal

³A Kolmogorov-Smirnov test reveals that our observed cumulative V distribution seen in Figure 9 is statistically indistinguishable from that of a single gaussian having $\mu = 2.9 \text{ km s}^{-1}$ and $\sigma = 1.7 \text{ km s}^{-1}$ (Table 6).

components having negative slope. The percentages indicate, however, that this is not the case— though we believe the detailed state of affairs to be satisfactory. The non-negligible off-diagonal elements are simply the result of tolerable bin “diffusion” of two types. First are cases where our use of photometric and abundance data has been able to resolve the Montes et al. (2001) uncertain memberships into affirmative or negative membership categories; this occurs for a substantial 34.4% of the total objects. Second are cases where our evaluation of the kinematics and use of photometric and abundance data in a conservative manner (assigning affirmative or negative membership only if this can be done at high confidence level) has moved the affirmative or negative kinematic membership assignments of Montes et al. (2001) to our uncertain category; this is a moderate affect only influencing 15.6% of the total objects.

The remaining two diagonal elements in the 3×3 contingency sub-table are more important. Only one star we finally classify as a member (2.7% of our members) is listed as a kinematic non-member by Montes et al. (2001); this is encouraging and speaks to the cleanliness of our final member sample. A modest 15.0% of our final non-members, however, are classified as kinematic members by Montes et al. (2001); these are HD 13594, 24160, 24916, 81659, 112196, and 167389. While this does not speak to the success of our primary goal in compiling a clean sample of UMa group members, it may suggest that our secondary goal of avoiding definitive misclassifications may not be fully met. Besides deviant kinematics, our photometry indicates non-membership for HD 81659 and strongly for 24160. Two kinematic components are deviant for both HD 24916 and 167389; the photometric criteria provide uncertain information here, and the activity of HD 167389 is low for an UMa member. We acknowledge, however, that the deviant U velocities seen for HD 13594 and 112196 would not exclude membership if we allowed real dispersion of only 4-5 km s⁻¹ (consistent with unbiased literature results in Table 6); moreover, HD 112196 is a probable activity-based member. Even if misclassified, these few cases are not intolerable. We have labeled final memberships of the latter two stars as N?/? so as not to relegate them to the obscurity of the general disk field, and deem the other 4 objects worthy of continued study (particularly for undetected companions and abundance determinations).

Tab. 7

4.3. Evidence of an Older Stream?

The outlying evolved stars in Figures 5 and 6 appear to form a well-defined sequence in the color-magnitude diagram. These objects (HD 745, 18645, 62668A, 81858A, 81858B, 88654 and 136901) are plotted again in Figure 10 with the same isochrones used in Figures 4-9. The two additional fiducials are 2 and 3 Gyr isochrones from the same Yale-Yonsei

set for solar metallicity and the Lejeune et al. (1998) color transformations. Comparison suggests that these evolved stars do form a genuine evolutionary sequence of uniform age. In their $d = 125$ pc volume-limited study of A-F stars, Chereul et al. (1999) noted with surprise the existence of ~ 2 Gyr old velocity structures discernible when employing coarse (velocity dispersions corresponding to 6.3 km s^{-1}) resolution filters. Are the objects in Figure 10 late-type members of these structures?

Fig. 10

In principle, kinematic assessment of alleged intermediate-age structures is difficult since the velocity components may not exhibit the relative coherence of younger structures such as UMa. Nevertheless, the UVW components of HD 745 and 88654 are indistinguishable within the uncertainties, as are the VW and UV components of HD 18645 and 62668A. Chereul et al. (1999) note a distinctive kinematic feature of their intermediate-aged streams is a positive and large (often $\geq 20 \text{ km s}^{-1}$) U component. Our evolved stars in Figure 10 show the same characteristic— *all* 6 systems have positive U with a mean of $+15 \text{ km s}^{-1}$. This kinematic characteristic is distinct in an absolute sense as well. The mean disk field defined by B, A, and F stars shows a mean U component of $\sim -12 \text{ km s}^{-1}$ (Asiain et al. 1999). Additionally, inspection of the disk field kernel density function and its projection in the UV plane at $W = 0$ (Figures 3 and 4 of Asiain et al. 1999; also their Figure 5) shows that the UV space occupied by our evolved late-type stars is otherwise poorly-populated. High-resolution spectroscopy could establish the chemical abundance uniformity of the objects in Figure 10, and thus address the question of the reality of such candidate old star streams.

4.4. Robustness of Activity as a Membership Criterion

The utility of activity measures to establish membership is illustrated by the results in Table 6 and Figures 5-7. Table 6 indicates a clear increase in all the velocity dispersions as one proceeds from probable activity-based members to possible activity-based members and then to activity-based non-members. This suggests some overall relation between membership and activity level. Inspection of the H-R diagrams too shows how the photometric scatter increases in moving from probable activity-based members to possible ones, and finally to activity-based non-members; again, this suggests a general relation between activity level and membership.

SM93 ask a more specific fundamental question: “is the use of chromospheric activity infallible for determining [UMa Group] membership?” Despite the results above, we believe the general answer is as one might expect— not unless all young disk stars are UMa Group members. However, the question above can be parsed into two distinct important ones: is chromospheric activity a reliable indicator of positive/negative membership? These can be

answered using the comparison of our activity-based classifications and our final membership assessments, presented as a contingency table in Table 8. A similar comparison utilizing the kinematic membership assessments of Montes et al. (2001) is shown in Table 9. Only a third of our probable (and possible as well) activity-based members are classed by us as final members; the results are the same (for both probable and possible activity-based members) utilizing the final membership assessments of Montes et al. (2001) as well. Half of our probable activity-based members and a quarter of our possible activity-based member samples are designated final non-members. Is this a failure in the use of chromospheric activity as a membership diagnostic? We believe this is not demonstrated since it may simply reflect a number of (presumably young) disk stars that are not UMa group members in our initial sample. In this light, our starting sample may simply be less clean than that of, e.g., SM93— though we note that 9 out of 11 of their possible activity-based members were assigned eventual kinematic-based non-membership by them.

Tab. 8
Tab. 9

The second more important question that SM93 were really asking is whether chromospheric activity can be used to exclude membership; a negative result here would have direct impact on the issue of age-activity correlations. Table 8 indicates that of our twenty-six activity-based non-members, only a single one (HD 38393) is classified as a final member. This suggests that activity, then, is a very robust discriminant of non-membership. Montes et al. (2001) classify three additional activity-based non-members (HD 167389, 184960, and 211575) as kinematic members, however. Indeed, the kinematics for the latter two of objects suggest possible membership; the only deviations are mild ones in U easily allowed if we had utilized the velocity dispersions from non-biased studies listed at the bottom of Table 6; moreover, kinematic membership would even be favored for HD 167389 utilizing these unbiased criteria. The photometric membership criteria, however, are inconclusive for all stars—this results in our final uncertain and probable non-membership assignments. Given these comparisons, we have listed final memberships of ?/Y? for HD 184960 and 21175, and a final membership of N?/? for HD 167389 in Table 5 for those interested in following up the present study with more definitive classifications as opposed to our primary goal of an ultra-clean member list. Even considering these four remarkable exceptions (15% of our activity-based non-members), activity remains a remarkably robust indicator of non-membership. The most pessimistic interpretation of our results we envision is that age-activity relations are best considered in a statistical sense due to the presence of (apparently infrequent) scatter.

4.5. UMa Group Chromospheric Activity

Residual chromospheric emission ($\log R'_{\text{HK}}$) is plotted against color for our final UMa members (filled symbols) in Figure 11. Values for HD 91480, 113139A, and 184960 (-4.47 , -4.48 , and -4.95 respectively) are deduced from the $\lambda 1335$ C II measures of Simon & Landsman (1991), the He I D₃ measures of Garcia Lopez et al. (1993), and the Mg II h&k measurement of Soderblom & Clements (1987); transformations to the Ca II H&K system were made using the regressions of Soderblom & Clements (1987) and the observed relations in Garcia Lopez et al. (1993). Also shown are the Pleiades, M34, and schematic Hyades data from Figure 3b. Several interesting notes can be made. First, the scatter in UMa activity is very small—comparable to that seen in the slightly older ($\sim 700 \pm 100$ Myr) Hyades, and considerably smaller than that seen in the younger Pleiades (~ 100 Myr) and M34 (~ 200 Myr) clusters. Second, the mean level of activity also appears indistinguishable from that in the Hyades. The former suggests that the young solar-type star decline in global activity levels and their star-to-star scatter must be relatively rapid, occurring sometime within 200–500 Myr. The latter observation is consistent with the revised similar UMa and Hyades ages—thus, the similarity of mean Hyades/UMa activity levels is perhaps not as remarkable as originally thought by Soderblom & Clements (1987); in this case, the (power law?) decline in chromospheric emission need not occur very close to the UMa/Hyades age.

Fig. 11

Given the small Hyades-like scatter in chromospheric emission in the UMa group, an interesting question is if the spread in rotation is also small, like that seen in the Hyades. Homogeneous rotational velocity determinations of a larger number of UMa members are needed to address this satisfactorily; unlike directly measured chromospheric emission values, *projected* rotational velocities require larger samples to develop a statistical picture on firm footing. However, the literature-based positions of a dozen or so UMa members in the $v \sin i$ –($B - V$) plane (see Figure 1 of SJF) reveals that: a) the majority of stars have Hyades or slightly *sub*-Hyades (projected) rotational velocities b) with the exception of HD 184960 ($v \sin i = 3 \text{ km s}^{-1}$ at $(B - V) = 0.492$, possibly anomalously low due to the unknown projection) and HD 115043 ($v \sin i = 25 \text{ km s}^{-1}$ at $(B - V) = 0.61$), the scatter appears comparable to that evinced by Hyades dwarfs or, in the extreme, perhaps intermediate to the rotational scatter shown by M34 and the Hyades (Figure 1 of SJF).

The lack of very low chromospheric emission (≤ -5.1 , say) in our UMa group members reinforces the conclusion of Soderblom & Clements (1987) that young stars having activity levels characteristic (in an absolute sense) of a Maunder-like minimum for the Sun are very rare. In comparison, the population of such very inactive field stars within 50 pc is estimated by Henry et al. (1996) to be 10%; follow-up high-resolution spectroscopic study now in preparation by JRK, ARV, and DRS suggests that indeed these objects are single, slowly

rotating stars significantly older than the Hyades. If, however, one defines the Maunder minimum-like phenomenon in a relative sense– e.g., a real sustained drop in $\log R'_{\text{HK}}$ by several tenths of a dex (e.g., Figure 7 of Henry et al. 1996) compared to a mean activity level– then three warm UMa stars seen in Figure 11 might be considered to be in such a phase. While assured membership is an issue for two of these objects, the fraction (12%) is consistent with the Henry et al. (1996) estimate for older solar neighborhood field stars. If true, this might suggest that solar-type stars spend 10% of nearly their entire main-sequence life in a period of abnormally low activity.

4.6. Trolling the Stream: Fishing for *bona fide* Unassured Members

4.6.1. Active Non- and Questionable Members

An interesting question is what is the nature of the Probable and Possible Activity-Based members that are not classified as final members? None appear to be members of other kinematic structures found in the analyses of Asiain et al. (1999) or Chereul et al. (1999), which typically have significant simultaneous negative U and V velocity components not characteristic of the active unassured members. If the velocity components and/or unbiased velocity dispersions from these studies are utilized, it is possible that roughly a third of these stars (HD 26913, 41593, 56168, 60491, 63433, 75935, 76218, 112196, 147513, 150706, and CG Cyg) are, in fact, *bona fide* UMa group members; this would include membership in perhaps related putative structures such as an extended Sirius branch or the new supercluster clumps lying near the Sirius supercluster in velocity phase space (Skuljan et al. 1999, Chereul et al. 1999). If not already final uncertain members, these stars are given dual N?/? assessments in Table 5; we note that HD 63433 and 75935 were found to be kinematic members, but their photometry prevented a positive final assessment.

Another third of the sample is characterized as belonging to close binary systems– thus their significant activity levels are not very remarkable. Many of the remaining one-third of active unassured UMa members are not well studied. It remains possible that these are additional rare examples of young field stars separated from apparent regions of recent star formation; regardless, additional high-resolution spectroscopic study is certainly warranted.

4.6.2. Photometric Members Near the UMa Turn-Off

The photometric membership criterion was noted to be most effective at eliminating non-members. Indeed, only two photometric non-members are considered kinematic mem-

bers here (HD 13959B and 156498A). Both are members of double systems, and their other component shows both consistent positive photometric and kinematic evaluations. Because we expect little-evolved UMa non-members to reside near the UMa main-sequence, photometry is not a generally robust method to assign positive membership. An exception is near the turn-off, where evolution off the zero-age main sequence makes a star’s residence near the UMa fiducial highly suggestive of (not merely consistent with) membership.

Such stars are abundant among our additional UMa candidate sample— their early spectral types probably precluding investigators from attempting activity measurements. Roughly 30 stars are present here with H-R diagram placement suggestive of membership, but whose kinematics were labeled N? or ?. An interesting feature of these stars is their generally significant and positive U values, which are not characteristic of the local young disk field or of other identified moving groups; the same intriguing feature is seen in our active but unassured members (above). Using the results of other unbiased kinematic studies as above, the stars HD 15144A, 50973, 56537, 77350, 79439, and 120818 would especially seem to be likely members. Inasmuch as there may be no such thing as a “normal” A star, precision detailed abundances will probably not be helpful in future assessments of these stars’ membership.

A. $H\alpha$ and Ca II IRT as Proxies for Ca II H&K

Revisiting Figures 1d (M34) and 2c (Pleiades) to now instead correct the Ca II IRT-based activity measures to an $H\alpha$ -based scale using equations 3-3 and 3-5 also yields seemingly much-improved results (shown in Figure 12) compared to those in Figures 1a and 2a. However, such a procedure only ensures self-consistency between the $H\alpha$ and Ca II IRT activity scales, and not absolute consistency with a true Ca II H&K scale. Figure 13 is analogous to Figure 3, but now shows the mean of the transformed $H\alpha$ - and *corrected* IRT-based $\log R'_{\text{HK}}$ values versus dereddened $(B - V)$ color. The filled circles are again the *directly measured* Pleiades H&K indices from Soderblom et al. (1993), and are connected to the transformed and corrected values for six stars in common.

A troubling feature of Figure 13 is that the majority of the coolest ($B - V \geq 1.0$) M34 and Pleiades stars show *transformed* R'_{HK} values that are considerably larger than *directly measured* values. Figures 1b and 2b suggests why. By now correcting the IRT-based values onto the $H\alpha$ scale, we have incorrectly selected the wrong index to correct, thus erroneously raising our activity measures by perhaps up to 0.5 dex for the coolest stars. That is, Figure 13 suggests that $H\alpha$ is not as reliable a tracer of the Ca II H&K index as the Ca II IRT lines for cool stars.

Fig. 12

Fig. 13

This is not unexpected on either observational or theoretical grounds since a) the transformations of Herbig (1985) were derived from early G-type stars, and b) the IRT features are subordinate lines connecting the upper 4 2P levels of the H&K lines with 3 2D metastable states. Moreover, it is well known that (in the framework of complete redistribution and detailed balance for the Lyman lines anyway) the NLTE $H\alpha$ source function is dominated by photoionization and recombination in solar-type stars (Cram & Mullan 1985). This contrasts with the Ca II lines, whose NLTE source function is dominated by collisional excitation and de-excitation. Curiously, we might expect the $H\alpha$ and Ca II H&K line source functions to show greater similarity in the cooler stars since photoionization is presumably becoming less important. However, the electron density will also determine if $H\alpha$ becomes collisionally-dominated like H&K in these stars; apparently, n_e is not high enough for this to occur—though it might in cooler M dwarfs (Fosbury 1974).

JRK and ARV are pleased to acknowledge support from NSF via grant AST-0086576 to JRK. ARV also gratefully acknowledges assistance from a Nevada Space Grant Consortium Scholarship, a Ronald McNair Fellowship, and NSF pass-through funding from a Western Alliance to Expand Student Opportunities scholarship while this work was carried out. AFG and SJA thank Dr. James E. Hesser, Director, Dominion Astrophysics Observatory, for the observing time on the 1.22-m telescope to obtain the spectrograms from which the radial velocities were measured. SJA acknowledges a grant from NASA used to support in part his work as a 1992 Hipparcos Guest Investigator.

REFERENCES

- Abt, H. A., & Levy, S. G. 1985, *ApJS*, 59, 229
- Adelman, S. J. 1988, *MNRAS*, 230, 671
- Andersen, J., Nordstrom, B., Ardeberg, A., Benz, W., Mayor, M., Imbert, M., Martin, N., Prevot, L., Lindgren, H., & Maurice, E. 1985, *A&AS*, 59, 15
- Asiain, R., Figueras, F., Torra, J., & Chen, B. 1999, *A&A*, 341, 427
- Barbier-Brossat, M., & Figon, P. 2000, *A&A*, 142, 217
- Bastian, U., & Roeser, S. 1998, *PPM Star Catalogue South* (Heidelberg: Spektrum Akad.)
- Bessell, M. S. 2000, *PASP*, 112, 961
- Binney, J., & Tremaine, S. 1987, *Galactic Dynamics*, (Princeton: Princeton University Press)

- Boesgaard, A. M., & Friel, E. D. 1990, *ApJ*, 351, 467
- Castellani, V., Degl’Innocenti, S., & Prada Moroni, P. G. 2001, *MNRAS*, 320, 66
- Cayrel de Strobel, G., Soubiran C., Friel E.D., Ralite N., Francois P. 1997, *A&AS*, 124, 299
- Cayrel de Strobel, G., Soubiran, C., & Ralite, N. 2001, *A&A*, 373, 159
- Chaboyer, B., Green, E.M., & Liebert, J. 1999, *AJ*, 117, 1360
- Chereul, E., Creze, M., & Bienayme, O. 1999, *A&AS*, 135, 5
- Cram, L. E., & Mullan, D. J. 1985, *ApJ*, 294, 626
- de Medeiros, J. R., & Mayor, M. 1999, *A&AS*, 139, 433
- de Medeiros, J. R., & Udry, S., *A&A*, 346, 532
- Delfosse, X., Forveille, T., Mayor, M., Burnet, M., & Perrier, C. 1999, *A&A*, 341, L63
- Duflot, M., Figon, P., & Meyssonnier, N. 1995, *A&A*, 114, 269
- Eggen, O J. 1992, *AJ*, 104, 1493
- Fabricius, C., & Makarov, V. V. 2000, *A&A*, 356, 141
- Fehrenbach, Ch, Duflot, M., Mannone, C, Burnage, R, & Genty, V. 1997, *A&AS*, 124, 255
- Fekel, F. K. 1991, in *IAU Transactions, Commission 30 report*, eds. D.W. Latham and R.P. Stefanik
- Fekel, F. C., Scarfe, C. D., Barlow, D. J., Duquenois, A., McAlister, H. A., Hartkopf, W. I., Mason, B. D., & Tokovinin, A. A. 1997, *AJ*, 113, 1095
- Fekel, F. C., Strassmeier, K. G., Weber, M., & Washuettl, A. 1999, *A&AS*, 137, 369
- Fosbury, R. A. E. 1974, *MNRAS*, 169, 147
- Gaidos, E. J., Henry, G. W., & Henry, S. M. 2000, *AJ*, 120, 1006
- Garcia Lopez, R., Rebolo, R., Beckman, J. E., & McKeith, C. D. 1993, *A&A*, 273, 482
- Green, E. M., Demarque, P., & King, C. R. 1987, *The Revised Yale Isochrones and Luminosity Functions*, (New Haven: Yale Univ. Obs.)

- Grenier, S., Burnage, R., Farraggiana R., Gerbaldi M., Delmas F., Gomez A.E., Sabas V., & Sharif L. 1999, A&AS, 135, 503
- Hauck, B., & Mermilliod, M. 1980, A&AS, 40, 1
- Herbig, G. H. 1985, ApJ, 289, 269
- Henry, T. J., Soderblom, D. R., Donahue, R. A., & Baliunas, S. L. 1996, AJ, 111, 439
- Hill, G., & Fisher, W.A. 1986, Publ. Dom. Astrophys. Obs., 16, 193
- Hildebrandt, G., Scholz, G., & Lehmann, H. 2000, AN, 321, 115
- Johnson, D. R. H., & Soderblom, D. R. 1987, AJ, 93, 864
- Jones, B. F., Fischer, D., Shetrone, M., & Soderblom, D. R. 1997, AJ, 114, 352
- Kurucz, R. L. 1993, in Peculiar Versus Normal Phenomena in A-Type and Related Stars, eds. M.M. Dworetsky, F. Castelli, R. Farragiana, ASP Conf. Ser., 44, 87
- Kurucz, R. L., & Avrett, E. H. 1991, Smithsonian Astrophys. Obs. Spec. Rep. 381
- Lejeune, Th., Cuisinier, F., & Buser, R. 1998, A&A, 130, 65
- Marcy, G. W., Lindsay, V., & Wilson, K. 1987, PASP, 99, 490
- Marcy, G. W., & Benitz, K. J. 1989, AJ, 344, 441
- Mermilliod, J.-C. 1981, A&A, 97, 235
- Meynet, G., Mermilliod, J.-C., & Maeder, A. 1993, A&AS, 98, 477
- Mihalas, D., & Binney, J. 1981, Galactic Astronomy, (San Francisco: W.H. Freeman and Company)
- Montes, D., Lopez-Santiago, J., Galvez, M. C., Fernandez-Figueroa, M. J., DeCastro, E., & Cornide, M. 2001, MNRAS, 328, 45
- Napiwotzki, R., Schonberger, D., & Wenske, V. 1993, A&A, 268, 653
- Nordstrom, B., Stefanik, R. P., Latham, D. W., & Andersen, J. 1997, A&AS, 126, 21
- Orlov, V.V., Panchenko, I. E., Rastorguev, A. S., & Yatsevich, A. V. 1995, Astron. Zh., 72, 495

- Perryman, M. A. C., Brown, A. G. A., Lebreton, Y., Gomez, A., Turon, C., Cayrel de Strobel, G., Mermilliod, J. C., Robichon, N., Kovalevsky, J., & Crifo, F. 1998, *A&A*, 331, 81
- Phelps, R. L. 1997, *ApJ*, 483, 826
- Pinsonneault, M. H., Stauffer, J. R., Soderblom, D. R., King, J. R., & Hanson, R. B. 1998, *ApJ*, 504, 170
- Popper, D. M. 1994, *AJ*, 108, 1091
- Poveda, A., Herrera, M. A., Allen, C., Cordero, G., & Lavalley, C. 1994, *RMxAA*, 28, 43
- Pudritz, R. E. 2002, *Sci*, 295, 68
- Rucinski, S. M. 1981, *AcA*, 31, 363
- Sarajedini, A., von Hippel, T., Kozhurina-Platais, V., & Demarque, P. 1999, *AJ*, 118, 2894
- Simon, T., & Landsman, W. 1991, *ApJ*, 380, 200
- Skuljan, J., Hearnshaw, J. B., & Cottrell, P. L. 1999, *MNRAS*, 308, 731
- Soderbloom, D. R., Mayor, M., 1993, *AJ*, 105, 226 (SM93)
- Soderblom, D. R., Jones, B. F., & Fischer, D. 2001, *ApJ*, 563, 334
- Soderblom, D. R., Stauffer, J. R., Hudon, J. D., & Jones, B. F. 1993, *ApJS*, 85, 315
- Soderblom, D. R. 1985, *AJ*, 90, 2103
- Soderblom, D. R., Duncan, D. K., Johnson, D. R. H. 1991, *ApJ*, 375, 722
- Soderblom, D. R., & Clements, S. D. 1987, *AJ*, 93, 920
- Soderblom, D. R., King, J. R., Hanson, R. B., Jones, B. F., Fischer, D., Stauffer, J. R., & Pinsonneault, M. H. 1998, *ApJ*, 504, 192
- Stickland, D. J., & Weatherby, J. 1984, *A&AS*, 57, 55
- Strassmeier, K. G., Fekel, F. C., Bopp, B. W., Dempsey, R. C., & Henry, G. W. 1990, *ApJS*, 72, 191
- Strassmeier, K. G., Washuettl, A., Granzer, T., Scheck, M., & Weber, M. 2000, *A&AS*, 142, 275

- Taylor, B.J. 2000, *A&A*, 362, 563
- Tokovinin, A. A., & Smekhov, M. G. 2002, *A&A*, 382, 118
- Weis, E. W. 1993, *AJ*, 105, 1962
- Weis, E. W. 1991, *AJ*, 101, 1882
- Wielen, R. 1971, *A&A*, 13, 309
- Wielen, R. 1991, in *The Formation and Evolution of Star Clusters*, ASP Conf. Ser., 13, 343
(San Francisco: ASP)
- Wielen, R. 1977, *A&A*, 60, 263
- Yi, S., Demarque, P., Kim, Y.-C., Lee, Y.-W., Ree, C. H., Lejeune, T., & Barnes, S. 2001, *ApJS*, 136, 417

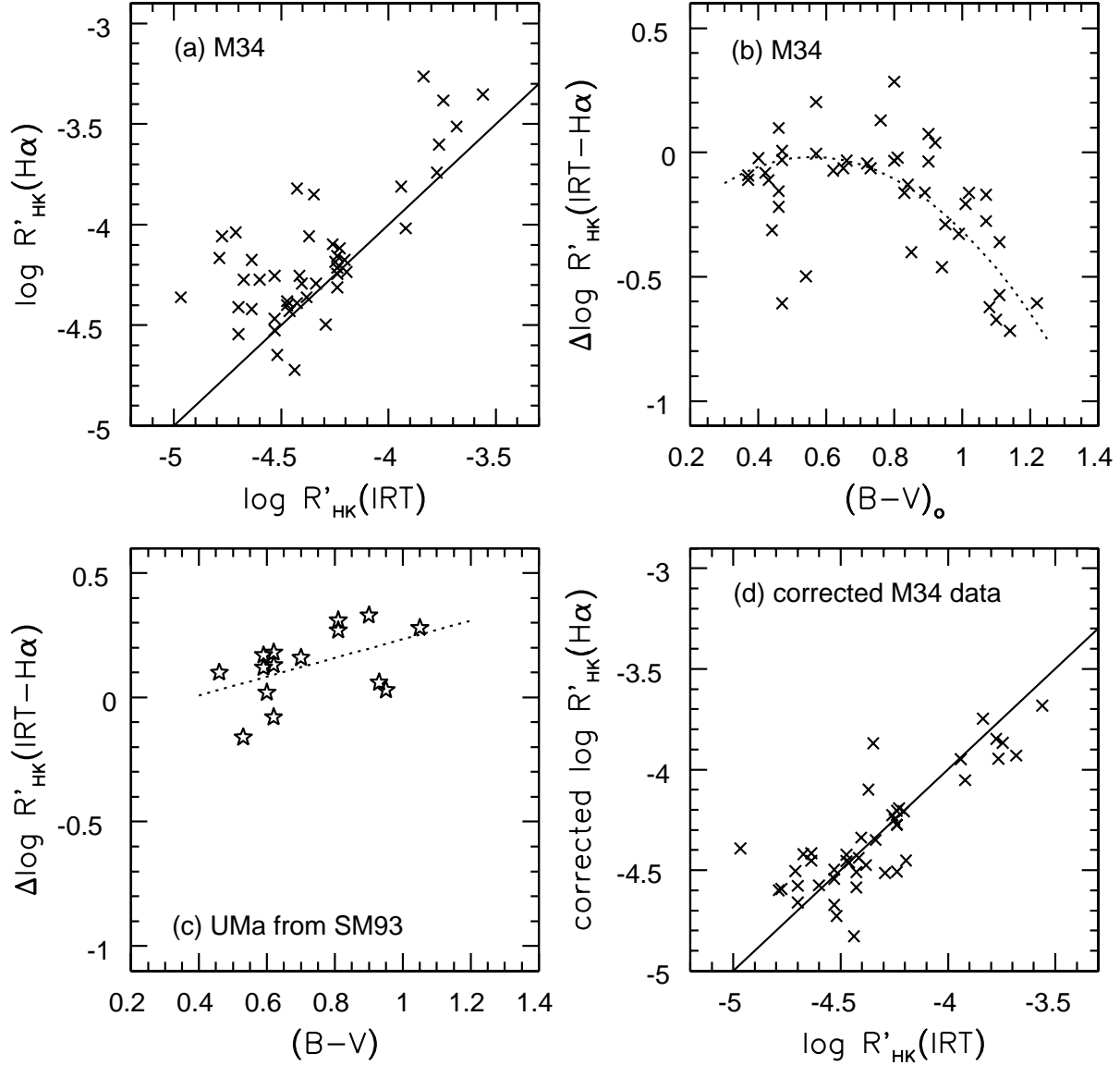


Fig. 1.— (a) Residual chromospheric fluxes (relative to photospheric) of the Ca II H&K lines as derived from the H α and Ca II infrared triplet lines utilizing the transformation in Herbig (1985) are compared for the sample of M34 (200 Myr) dwarfs from Soderblom et al. (2001); the solid line depicts an identical relationship. (b) The difference between the H α - and Ca II IRT-based residual fluxes is plotted against color; the dotted line is a quadratic fit to the data. (c) The differenced residual chromospheric fluxes for UMa candidate stars from SM93; the dotted line is a least squares linear fit. (d) The same as panel (a) except the H α -based residual fluxes on the ordinate have been corrected using the fitted relation in panel (b).

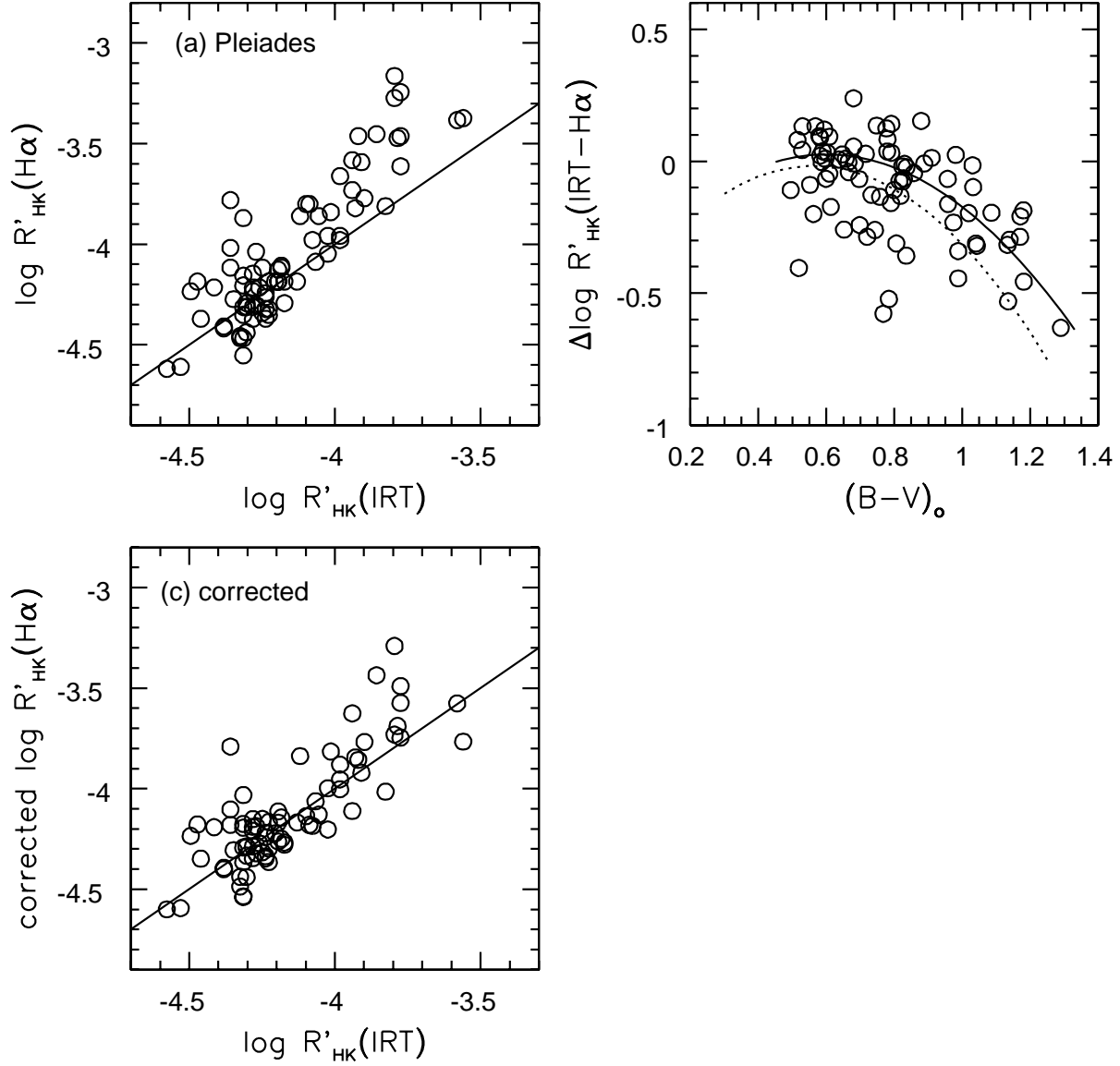


Fig. 2.— (a) The same as Figure 1a, except for Pleiades dwarf data from Soderblom et al. (1993). (b) The same as Figure 1b, except for Pleiades dwarfs. The solid line is the fitted quadratic Pleiades relation; the dotted line is the fit to the M34 data from Figure 1b. (c) The same as Figure 1(d), except for Pleiades dwarfs with their $\text{H}\alpha$ -based residual fluxes corrected by the fitted relation (equation 3-5) in (b).

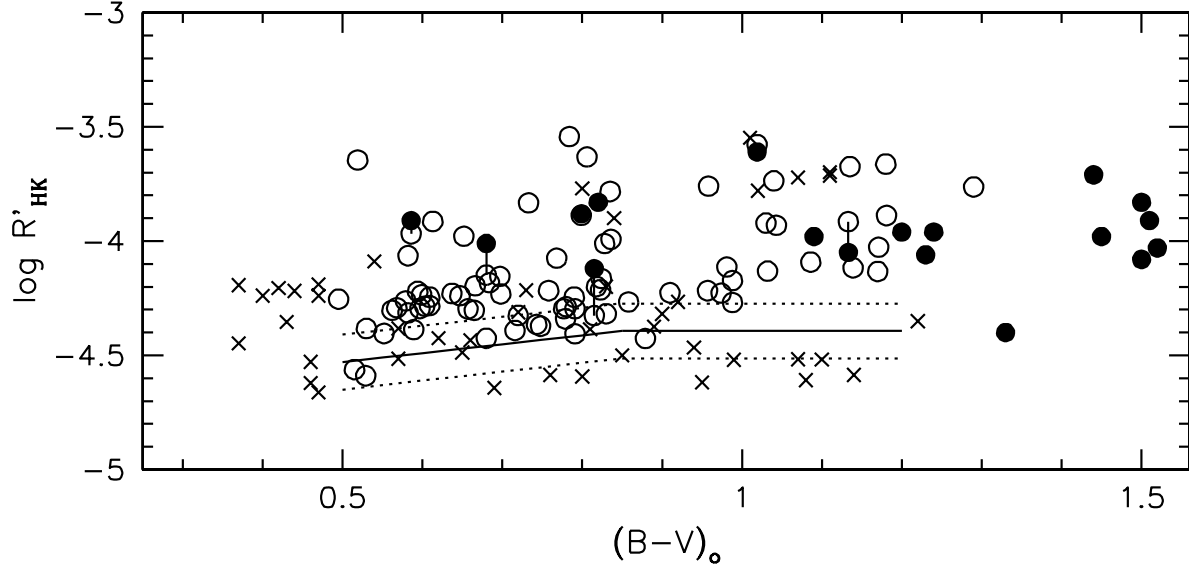


Fig. 3.— Residual chromospheric flux in Ca II H&K versus $(B - V)$ color. The crosses are the averaged IRT- and corrected (as in Figure 2d) $H\alpha$ -based data for M34 dwarfs (from Soderblom et al. 2001) transformed to Ca II H&K using the relations from Herbig (1985). The open circles are similar data for Pleiades dwarfs from Soderblom et al. (1993) shown in Figure 2; closed circles are *actual* H&K Pleiades measurements from Soderblom et al. (1993), and are connected to the averaged transformed $H\alpha$ - and IRT-based values by vertical lines. The solid and dotted lines shown the mean Hyades relation and full extent of its scatter from Soderblom (1985).

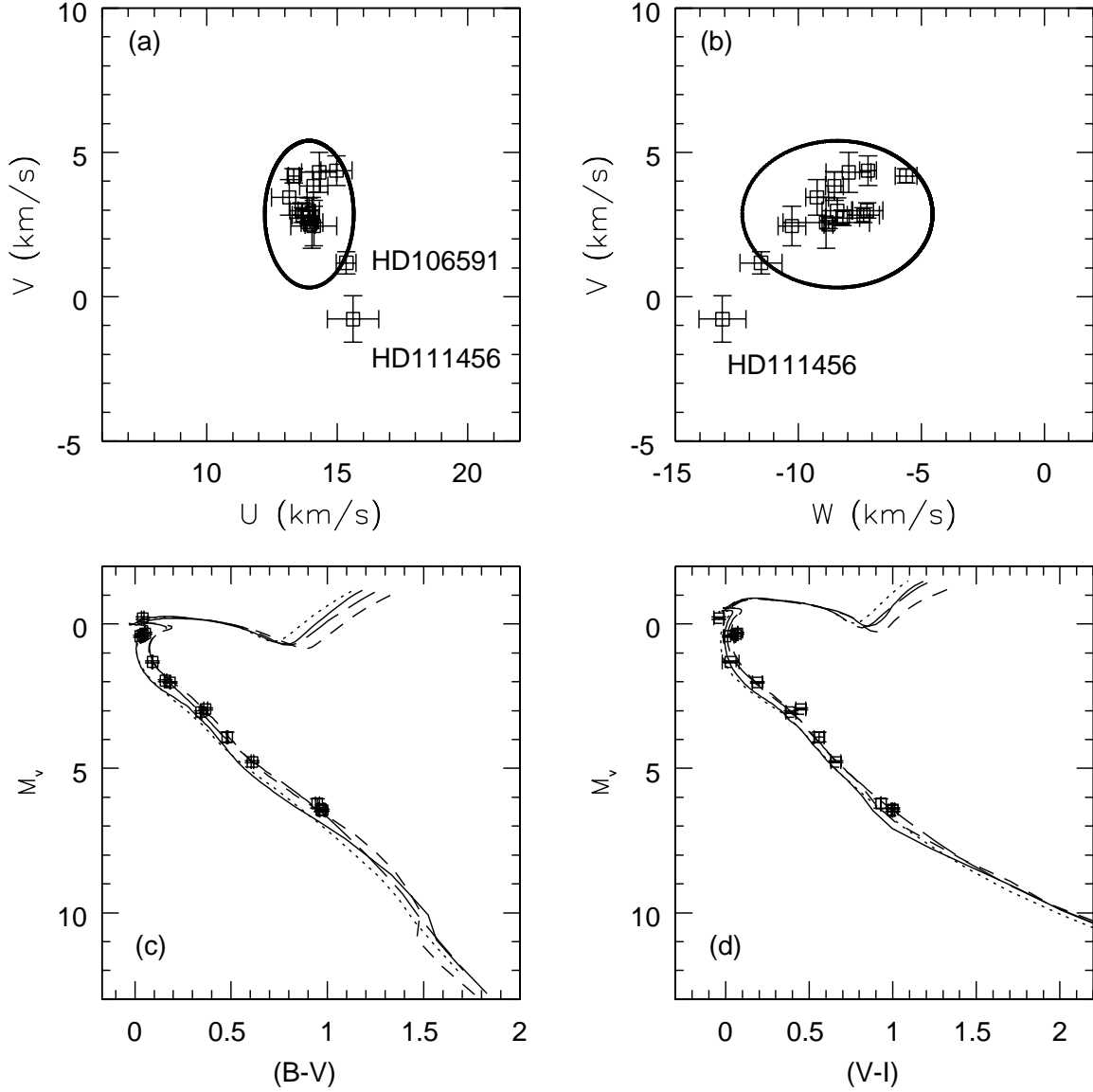


Fig. 4.— (a) UMa nucleus stars in the V - U kinematic plane; the ellipse denotes three times the velocity dispersion. (b) UMa nucleus stars in the V - W plane with the 3σ velocity dispersion ellipse. (c) UMa nucleus stars in the *Hipparcos*-based M_V -($B-V$) HR diagram. The lines are the newest Yale isochrones (Yi et al. 2001) for 600 Myr. Plotted are: the Lejeune et al. (1998) color transformation-based isochrones for $Z=0.01$ (solid line) and 0.02 (short dashed line); and the Green et al. (1987) color transformation-based isochrones for $Z=0.01$ (dotted line) and 0.02 (long dashed line). (d) The UMa nucleus M_V -($V-I$) H-R diagram with the same isochrones, but for a 400 Myr age.

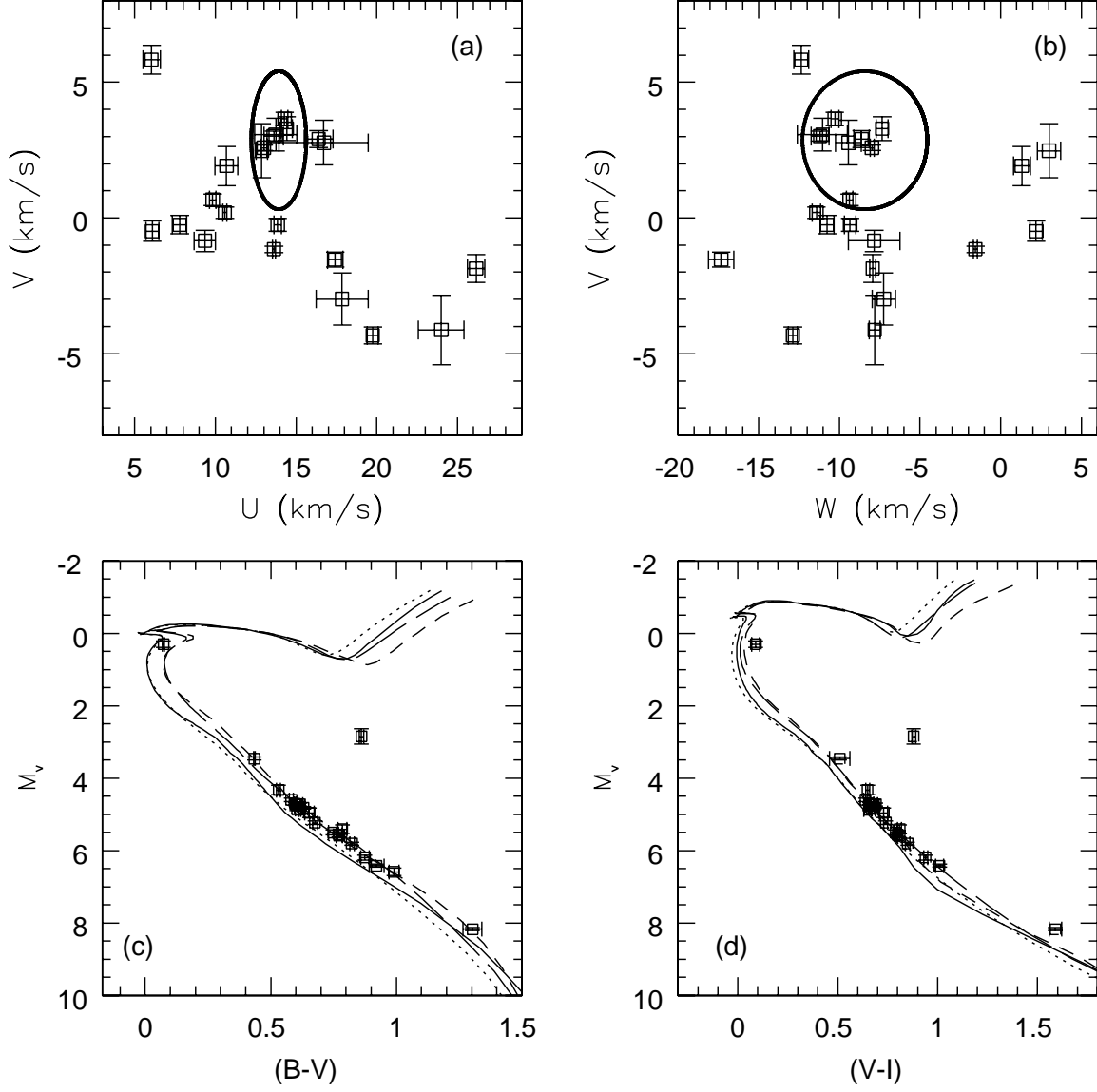


Fig. 5.— Same as Figure 4, but for the probable activity-based UMa group members. The velocity ellipses are those from the UMa nucleus stars.

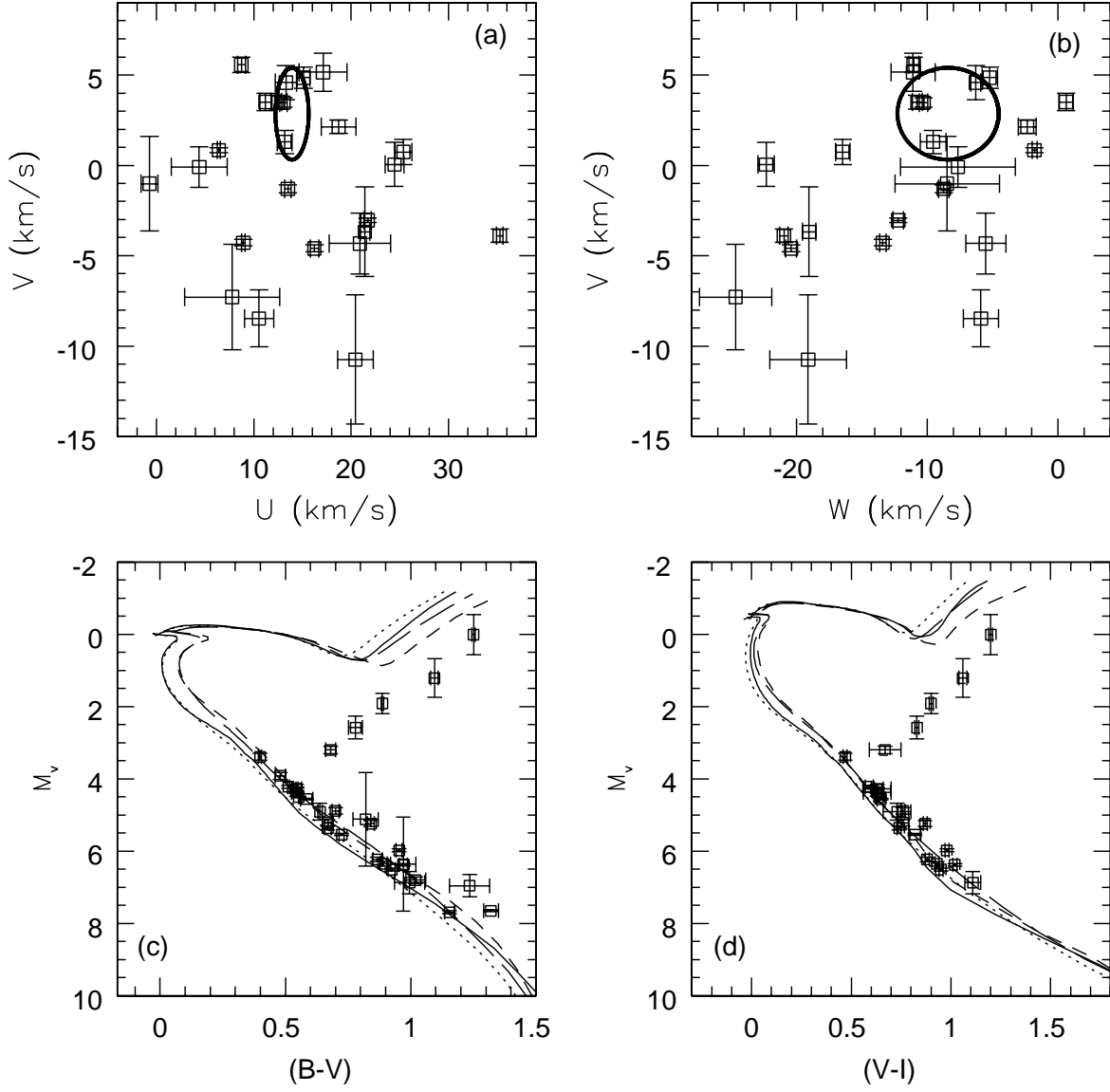


Fig. 6.— Same as Figure 5, but for the possible activity-based UMa group members.

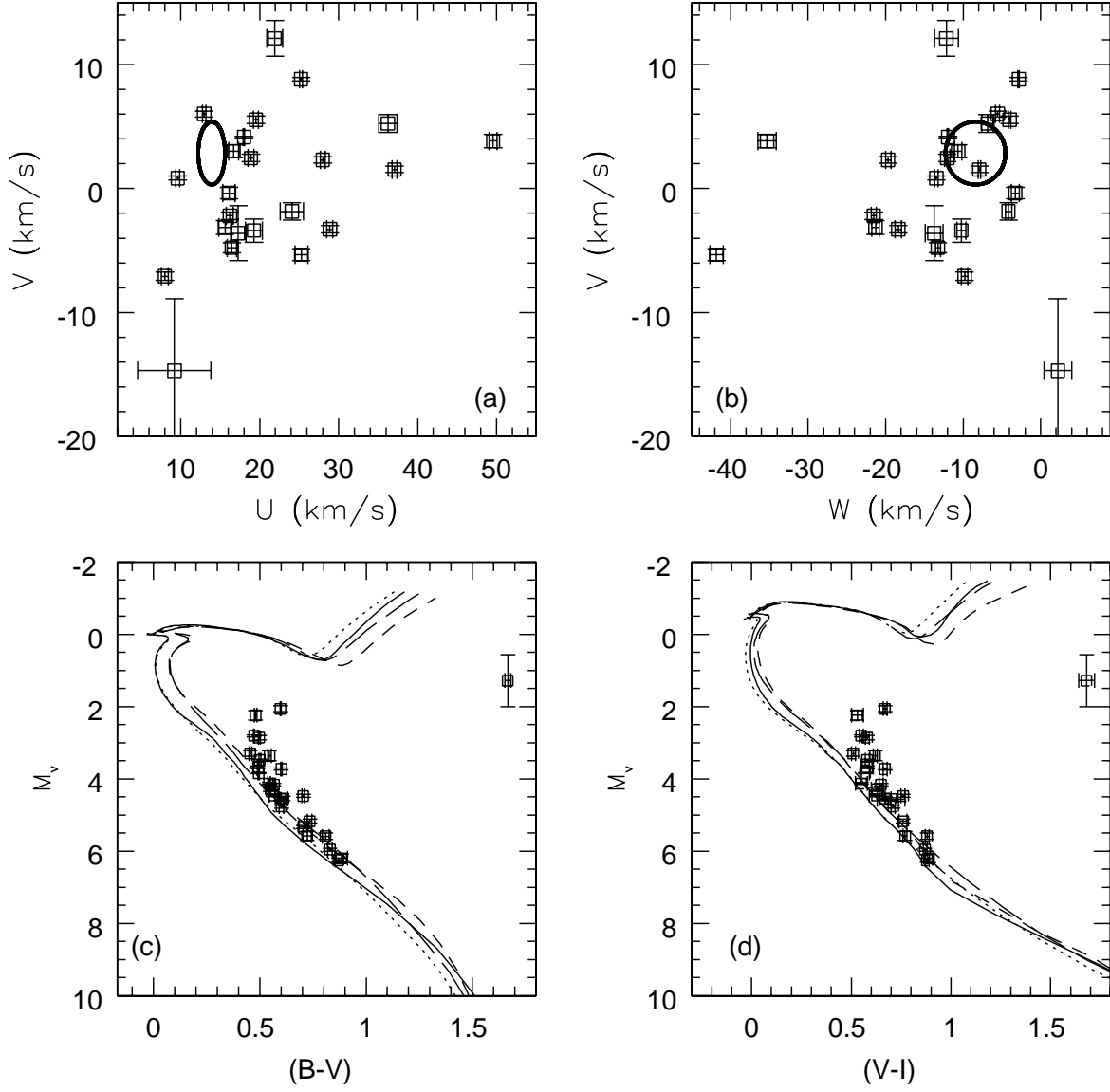


Fig. 7.— Same as Figure 5, but for the probable activity-based UMa group non-members.

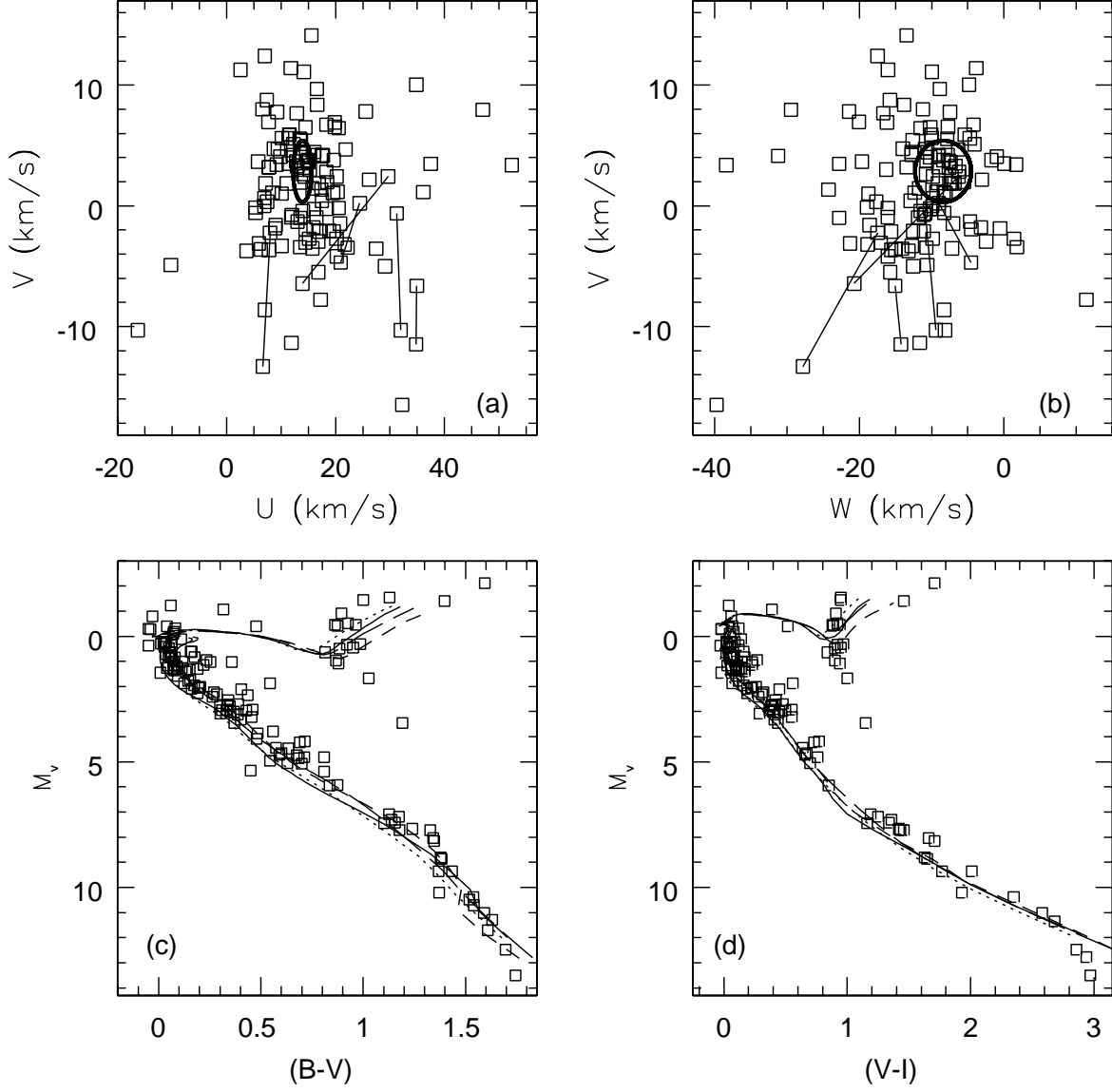


Fig. 8.— Same as Figure 5, but for the additional UMa group candidates lacking activity measures. Error bars have been omitted for clarity.

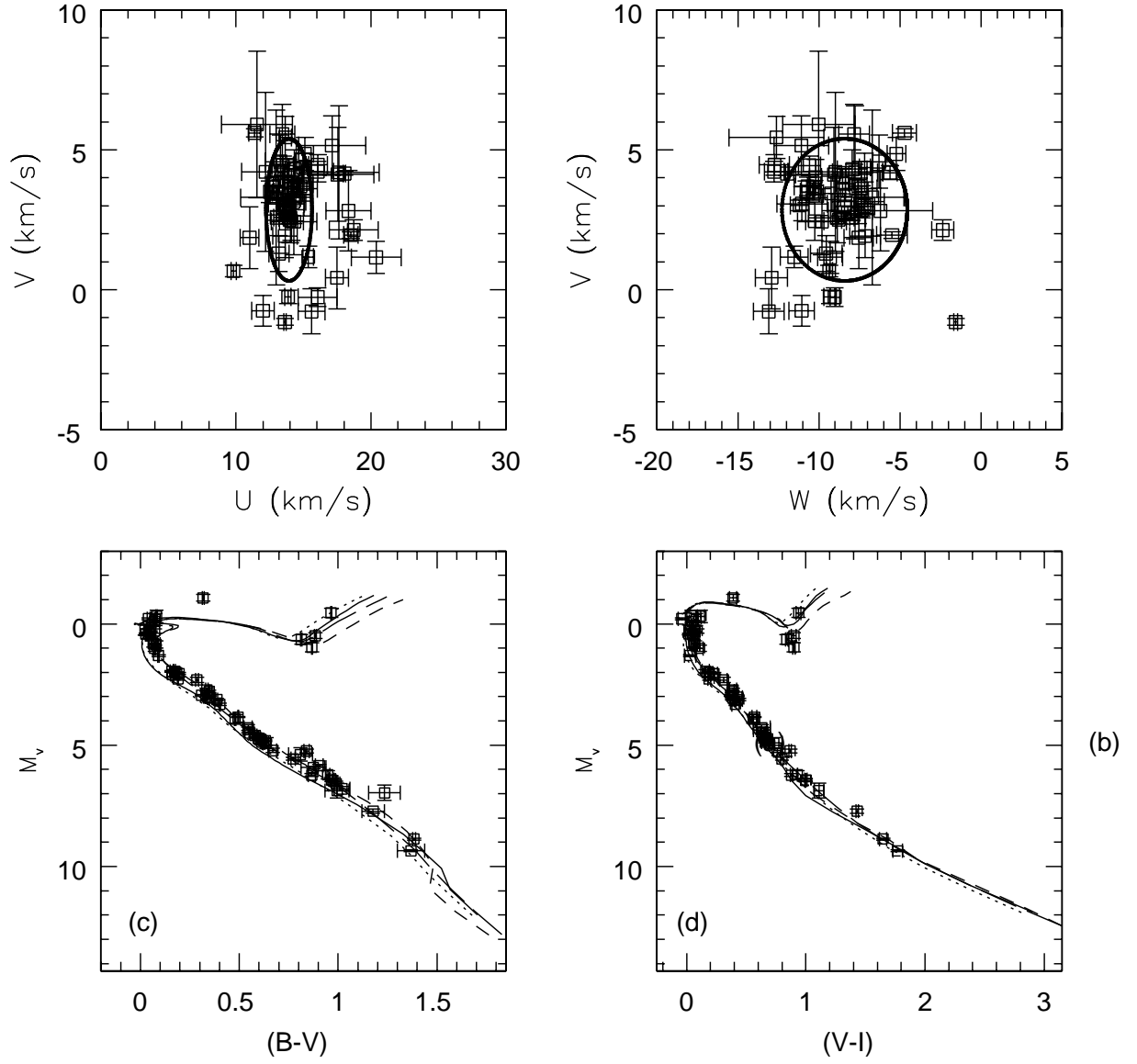


Fig. 9.— Same as Figure 5, but for our final probable and possible UMa group members.

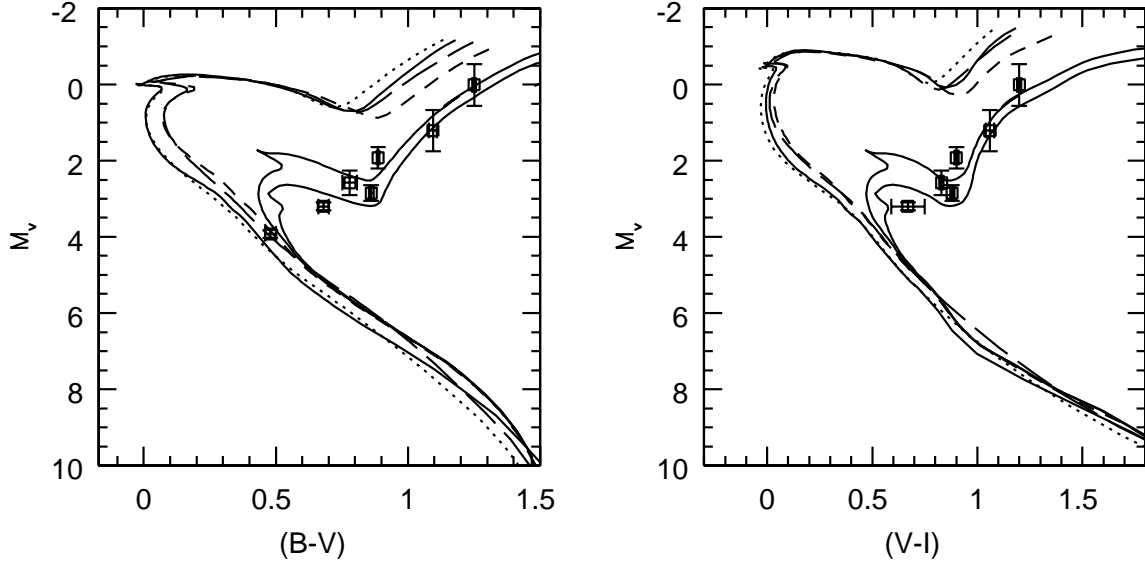


Fig. 10.— Color-magnitude diagrams of outlying evolved stars from Figures 5 and 6 and the same 400 and 600 Myr Yale-Yonsei isochrones plotted in Figures 4-9; the two older fiducials are 2 and 3 Gyr Yale-Yonsei isochrones.

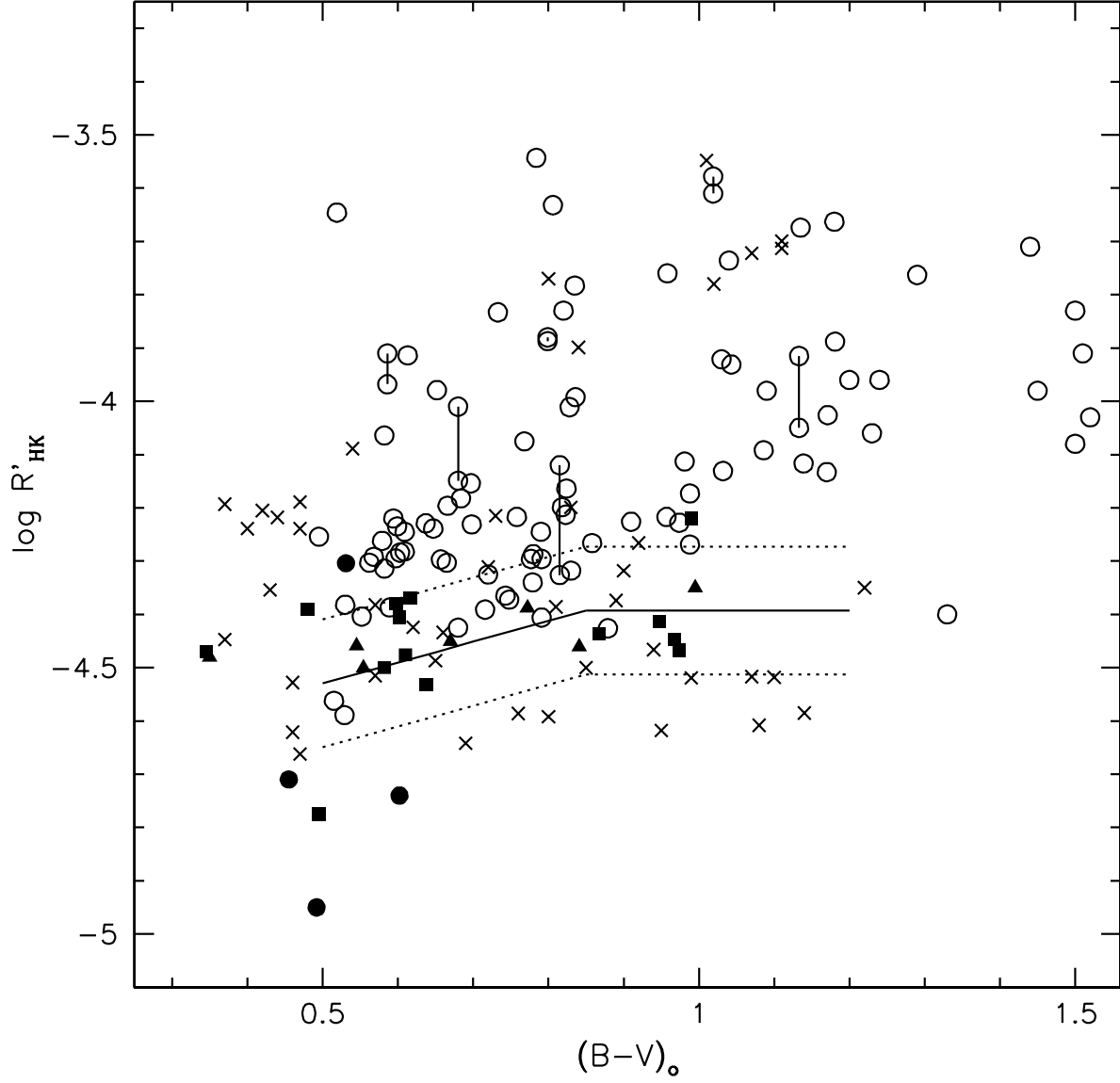


Fig. 11.— The chromospheric emission-color plane with the Hyades relation (lines), M34 data (crosses), and Pleiades data (open circles only) from Figure 3. The filled squares are our final probable and possible UMa group members (single or wide binaries). Filled triangles are final probable and possible members that are spectroscopic binaries, close visual binaries, or known active variables. Filled circles are four kinematic members from Montes et al. (2001) that are indeed likely UMa group members, but are not within our final clean member sample.

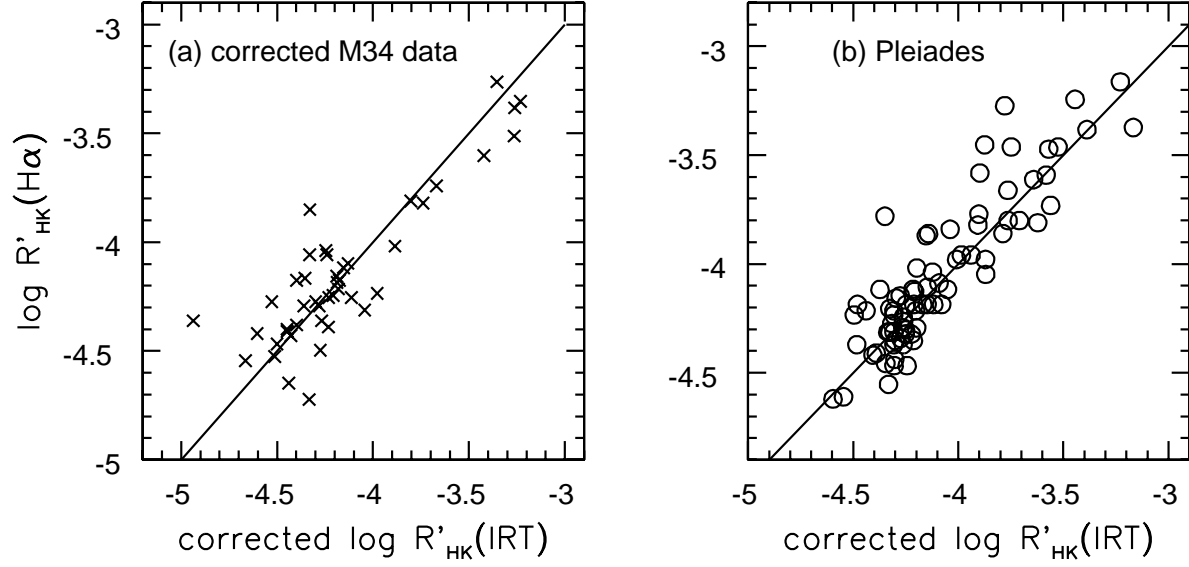


Fig. 12.— Same as Figures 1d and 2c, respectively, except IRT-based activity measures have been corrected to an H α -based scale utilizing equations 3-3 and 3-5.

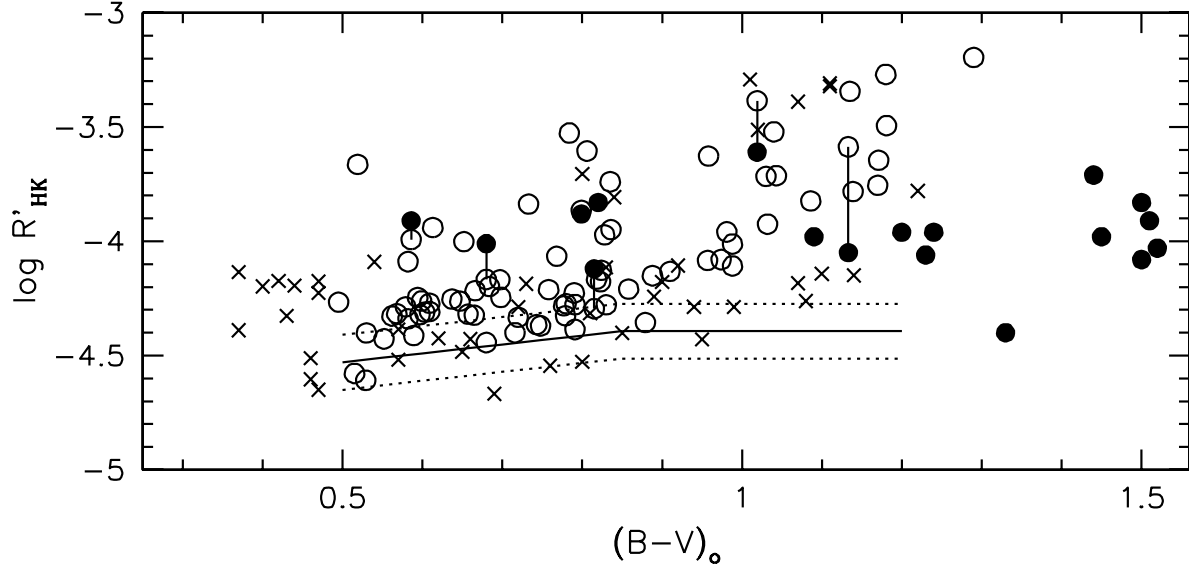


Fig. 13.— Same as Figures 3 except the Pleiades and M34 chromospheric fluxes are from averaged $H\alpha$ - and corrected Ca II IRT-based transformations.